TKK Reports in Forest Products Technology, Series A4
Espoo 2008

PROPERTIES AND INTERFACIAL BEHAVIOUR OF CELLULOSE NANOFIBRILS

Doctoral Thesis

Susanna Ahola

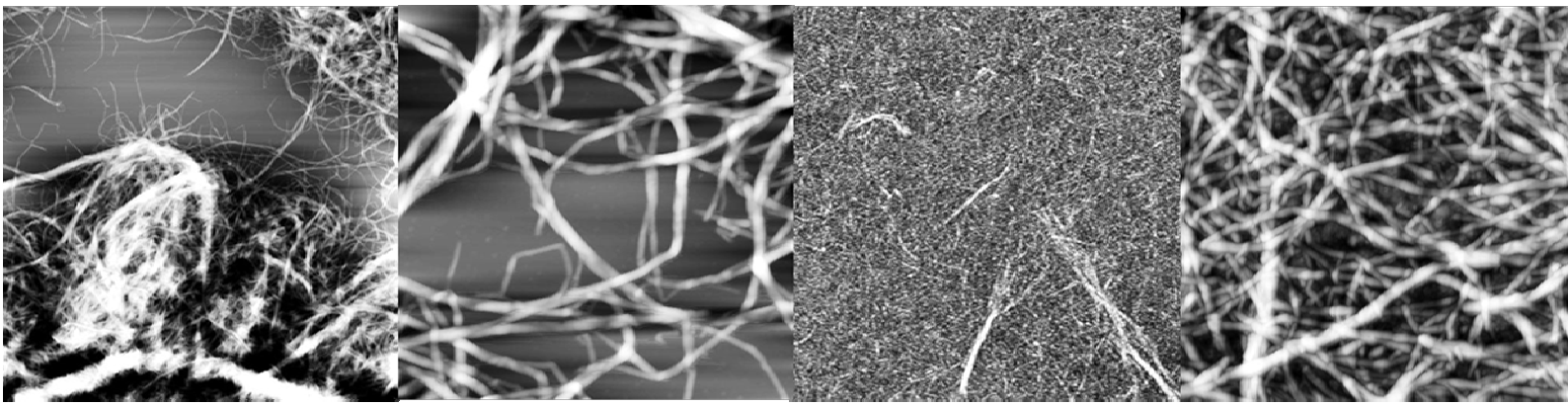

TEKNILLINEN KORKEAKOULU
TEKNISKA HÖGSKOLAN
HELSINKI UNIVERSITY OF TECHNOLOGY
TECHNISCHE UNIVERSITÄT HELSINKI
UNIVERSITE DE TECHNOLOGIE D'HELSINKI

TKK Reports in Forest Products Technology, Series A4
Espoo 2008

PROPERTIES AND INTERFACIAL BEHAVIOUR OF CELLULOSE NANOFIBRILS

Doctoral Thesis

Susanna Ahola

Dissertation for the degree of Doctor of Science in Technology to be presented with due permission of the Faculty of Chemistry and Materials Sciences for public examination and debate in Auditorium Puu II at Helsinki University of Technology (Espoo, Finland) on the 5th of December, 2008, at 12 noon.

Helsinki University of Technology
Faculty of Chemistry and Materials Sciences
Department of Forest Products Technology

Teknillinen korkeakoulu
Kemian ja materiaalitieteiden tiedekunta
Puunjalostustekniikan laitos

Distribution:
Helsinki University of Technology
Faculty of Chemistry and Materials Sciences
Department of Forest Products Technology
P.O. Box 6300
FIN-02015 TKK

ISBN 978-951-22-9648-4 (printed)
ISSN 1797-4496
ISBN 978-951-22-9649-1 (PDF)
ISSN 1797-5093
URL: http://lib.tkk.fi/Diss/2008/isbn9789512296491/

Picaset Oy
Helsinki 2008

ABSTRACT OF DOCTORAL DISSERTATION	HELSINKI UNIVERSITY OF TECHNOLOGY P.O. BOX 1000, FI-02015 TKK http://www.tkk.fi

Author Susanna Ahola

Name of the dissertation
Properties and interfacial behaviour of cellulose nanofibrils

Manuscript submitted August 29, 2008	Manuscript revised November 11, 2008
Date of the defence December 5, 2008	
☐ Monograph	☒ Article dissertation (summary + original articles)

Faculty	Faculty of Chemistry and Materials Sciences
Department	Department of Forest Products Technology
Field of research	Forest Products Chemistry
Opponent(s)	Professor Derek Gray
Supervisor	Professor Janne Laine
Instructor	Docent Monika Österberg

Abstract

The properties and interfacial behaviour of cellulose nanofibrils were studied using cellulose model surfaces and surface methods such as quartz crystal microbalance with dissipation (QCM-D) and atomic force microscopy (AFM). The overall aim of the work was to characterise cellulose nanofibril materials, and to study the interactions of the nanofibrils with water, polymers and enzymes in order to understand the behaviour of nanofibrils in future nanotechnology applications.

Nanofibrils were prepared from delignified pulp fibres using an enzymatic pre-treatment combined with mechanical shearing, followed by disintegration in a homogenizer. The procedure resulted in high-aspect-ratio nano-scale fibrils with a width of about 5 nm and a length up to several micrometers. The high-aspect-ratio nanofibrils were found to form an entangled network which under aqueous conditions forms high-water-content gel-like structures.

Cellulose nanofibril model films were prepared by spin-coating aqueous nanofibril dispersions on silica substrates. These model surfaces were further utilised to study the interactions of the nanofibrils with water, enzymes and polymers. The interactions of the nanofibrils were shown to be similar to the interactions of cellulosic fibres, but the gel-like structure and large specific surface area of the nanofibrils affected many interfacial phenomena of nanofibrils, such as swelling, surface forces, enzymatic degradability, and the adsorption of polymers on nanofibril surfaces.

Polymer adsorption on cellulose nanofibril surfaces was found to be highly dependent on the nature of nanofibril/polymer interaction. Adsorption of a neutral polysaccharide caused a dispersing effect of the nanofibrils and water uptake in the film, whereas adsorption of a cationic polyelectrolyte caused water removal and densification of the film. Choosing the right type of polymer interaction is essential for further applications where polymers and nanofibrils are mixed together.

The potential of cellulose nanofibrils as a strength reinforcing agent was demonstrated by using nanofibrils together with a cationic polyelectrolyte to enhance paper strength. The paper strength experiments together with fundamental interaction studies showed that the use of nanofibrils as a strength reinforcement agent together with a cationic polyelectrolyte leads to significant improvements in paper strength properties.

Keywords cellulose nanofibril, model surface, swelling, polymer adsorption

ISBN (printed)	978-951-22-9648-4	ISSN (printed)	1797-4496
ISBN (pdf)	978-951-22-9649-1	ISSN (pdf)	1797-5093
Language	English	Number of pages	74 p. + app. 62 p.

Publisher Helsinki University of Technology, Department of Forest Products Technology

Print distribution Helsinki University of Technology, Department of Forest Products Technology

☒ The dissertation can be read at http://lib.tkk.fi/Diss/

VÄITÖSKIRJAN TIIVISTELMÄ	TEKNILLINEN KORKEAKOULU PL 1000, 02015 TKK http://www.tkk.fi

Tekijä Susanna Ahola

Väitöskirjan nimi
Nanofibrillaarisen selluloosan ominaisuudet ja pintavuorovaikutukset

Käsikirjoituksen päivämäärä 29.8.2008	Korjatun käsikirjoituksen päivämäärä 11.11.2008
Väitöstilaisuuden ajankohta 5.12.2008	
☐ Monografia	☒ Yhdistelmäväitöskirja (yhteenveto + erillisartikkelit)

Tiedekunta	Kemian ja materiaalitieteiden tiedekunta
Laitos	Puunjalostustekniikan laitos
Tutkimusala	Puunjalostuksen kemia
Vastaväittäjä(t)	Professori Derek Gray
Työn valvoja	Professori Janne Laine
Työn ohjaaja	Dosentti Monika Österberg

Tiivistelmä
Selluloosan nanofibrillien ominaisuuksia ja pintakäyttäytymistä tutkittiin käyttäen selluloosan mallipintoja ja pintamenetelmiä, kuten kvartsikidemikrovaakaa (QCM-D) ja atomivoimamikroskopiaa (AFM). Työn tarkoitus oli karakterisoida selluloosananofibrillimateriaaleja ja tutkia nanofibrillien ja eri aineiden, kuten veden, polymeerien ja entsyymien, välisiä vuorovaikutuksia. Tavoitteena oli ymmärtää nanofibrillien käyttäytymistä mahdollisissa nanoteknologian sovelluksissa.
Nanofibrillejä valmistettiin valkaistuista sellukuiduista käyttäen entsymaattista kuitujen esikäsittelyä, joka yhdistettiin mekaaniseen esikäsittelyyn ennen lopullista kuitujen hajotusta homogenisaattorissa. Tällä menetelmällä saatiin tuotettua korkean muotosuhteen nanofibrillejä, joiden leveys oli noin 5 nm ja pituus jopa useita mikrometrejä. Osoitettiin, että nämä nanofibrillit muodostavat kietoutuneita verkostorakenteita ja vedessä nämä kietoutuneet fibrillit muodostavat runsaasti vettä sisältäviä geelirakenteita.
Nanofibrilleistä valmistettiin mallipintoja päällystämällä piidioksidi-pintoja nanofibrilli-vesidispersiolla. Nämä mallipinnat karakterisoitiin ja niitä hyödynnettiin nanofibrillien vuorovaikutustutkimuksissa. Nanofibrillien vuorovaikutukset olivat samankaltaisia kuin sellukuitujen vuorovaikutukset, mutta fibrillien geelimäinen rakenne ja suuri ominaispinta-ala vaikuttivat useisiin pintakemiallisiin ilmiöihin, kuten turpoamiseen, pintavoimiin, entsymaattiseen hajoamiseen ja polymeerien adsorptioon.
Polymeerien adsorptio nanofibrillien pinnalle oli vahvasti riippuvainen nanofibrillien ja polymeerien välisestä vuorovaikutuksesta. Neutraalin polysakkaridin adsorptio aiheutti materiaalin dispergoitumista ja veden sitoutumista materiaaliin. Kationisen polyelektrolyytin adsorptio aiheutti veden poistumista materiaalista ja pinnan tiivistymisen. Oikeanlaisen nanofibrilli/polymeeri-vuorovaikutuksen valitseminen on oleellista tulevaisuuden sovelluksissa, joissa polymeerejä ja nanofibrillejä sekoitetaan keskenään.
Selluloosan nanofibrillien potentiaali lujuutta parantavana lisäaineena osoitettiin käyttämällä nanofibrillejä yhdessä kationisen polyelektrolyytin kanssa lisäämään paperin lujuutta. Paperin lujuusmääritykset yhdistettynä perustutkimuksellisiin vuorovaikutustutkimuksiin osoittivat, että nanofibrillien käyttö yhdessä kationisen polyelektrolyytin kanssa johtaa merkittäviin parannuksiin paperin lujuusominaisuuksissa.

Asiasanat Nanofibrillarinen selluloosa, mallipinta, turpoaminen, polymeerien adsorptio, paperin lujuus

ISBN (painettu)	978-951-22-9648-4	ISSN (painettu)	1797-4496
ISBN (pdf)	978-951-22-9649-1	ISSN (pdf)	1797-5093
Kieli	englanti	Sivumäärä	74 s. + liit. 62 s.
Julkaisija	Teknillinen Korkeakoulu, Puunjalostustekniikan laitos		

Painetun väitöskirjan jakelu Teknillinen Korkeakoulu, Puunjalostustekniikan laitos

☒ Luettavissa verkossa osoitteessa http://lib.tkk.fi/Diss/

PREFACE

This study was carried out in the Department of Forest Products Technology at Helsinki University of Technology during 2004-2008. The work was performed as a part of the "Nanostructured cellulose products" project in the Finnish-Swedish Wood Material Science research program and the "Designed cellulosic nanostructures" project in the European WoodWisdom-Net research program. All the funding and research parties of these projects are gratefully acknowledged for their contribution. Tom Lindström and Mikael Ankerfors from STFI-Packforsk are especially thanked for providing the nanocellulose materials throughout the work.

I am grateful to my supervisor Professor Janne Laine for giving me this inspiring topic to work with and for his guidance and insights throughout the work. My advisor Docent Monika Österberg is gratefully acknowledged for supervising my scientific writing, teaching me the details of AFM imaging, and most of all, being there for me daily. I would also like to thank Professor emeritus Per Stenius for introducing me to the exciting world of surface and colloid chemistry.

I have been privileged to work with top-class scientists throughout the research. I am humbly grateful to all my co-authors: Marjo Pääkkö, Mikael Ankerfors, Harri Kosonen, Antti Nykänen, Janne Ruokolainen, Per T. Larsson, Olli Ikkala, Tom Lindström, Jani Salmi, Leena-Sisko Johansson, Petri Myllytie, Tuija Teerinen, Xavier Turon, and Orlando J. Rojas, for fruitful co-operation. Lars Wågberg and Christian Aulin from KTH are also thanked for co-operation. Professors Maija Tenkanen and Mark Rutland are acknowledged for their constructive comments on the thesis.

It is difficult to think of a superlative strong enough to describe the gratitude that I feel for all my past and present colleagues in the former Laboratory of Forest Products Chemistry at TKK. The working atmosphere has been inspiring but also enjoyable during all these years and I can not imagine ever working in a nicer atmosphere than we had. Ritva Kivelä, Marja Kärkkäinen and Aila Rahkola are thanked for their skilful experimental assistance. Eero Kontturi is thanked for many valuable discussions. Riitta Hynynen and Ritva Vuorinen are thanked for taking care of many practicalities. Our librarian Kati Mäenpää is thanked for her help in literature acquisitions. Juha Lindfors is thanked for his help with the thesis layout, and especially for his inspiring friendship. The "Joyful Coffee Group" is thanked for many memorable not-so-work-related moments, with special thanks to Juha, Tuula, Petri, Miro, and Katri. All members of The Bloody Unstable Colloids singing group are also thanked for many unforgettable moments.

My deepest thanks go to my family and friends for their support throughout my life. And finally, my most loving thanks to my husband Mikko Ahola for spending many weekends in the laboratory with me, for proof-reading the thesis, and most of all, for his endless love, support and belief in me.

Espoo, November 12th, 2008

Susanna Ahola

LIST OF PUBLICATIONS

This thesis is mainly based on the results presented in five publications which are referred to as Roman numerals in the text. Some additional unpublished data are also related to the work.

Paper I Pääkkö, M., Ankerfors, M., Kosonen, H., Nykänen, A., Ahola, S., Österberg, M., Ruokolainen, J., Laine, J., Larsson, P.T., Ikkala, O., Lindström, T. (2007) Enzymatic hydrolysis combined with mechanical shearing and high-pressure homogenization for nanoscale cellulose fibrils and strong gels. *Biomacromolecules* 8: 1934-1941.

Paper II Ahola, S., Salmi, J., Johansson, L.-S., Laine, J., Österberg, M. (2008) Model films from native cellulose nanofibrils. Preparation, swelling, and surface interactions. *Biomacromolecules* 9: 1273-1282.

Paper III Ahola, S., Myllytie, P., Österberg, M., Teerinen, T., Laine, J. (2008) Effect of polymer adsorption on cellulose nanofibril water binding capacity and aggregation. *BioResources* 3(4): 1315-1328.

Paper IV Ahola, S., Österberg, M., Laine, J. (2008) Cellulose nanofibrils – adsorption with poly(amideamine) epichlorohydrin studied by QCM-D and application as a paper strength additive. *Cellulose* 15: 303-314.

Paper V Ahola, S., Turon, X., Österberg, M., Laine, J., Rojas, O. (2008) Enzymatic hydrolysis of native cellulose nanofibril and other cellulose model films – Effect of surface structure. *Langmuir* 24(20): 11592-11599.

Author's contribution to the appended joint publications:

I Susanna Ahola participated in defining the research plan with the co-authors, performed the AFM experiments, analysed the experimental results, and wrote the corresponding chapter in the manuscript.

II-V Susanna Ahola was responsible for the experimental design, performed the main part of the experimental work, analysed the corresponding results, and wrote main part of the manuscript.

LIST OF ABBREVIATIONS

AFM	atomic force microscopy
APTS	3-aminopropyltrimethoxysilane
BC	bacterial cellulose
CLSM	confocal laser scanning microscopy
CMC	carboxymethyl cellulose
DLVO	Derjaguin-Landau-Verwey-Overbeek theory
DMAc-LiCl	dimethylacetamide with lithium chloride
HC	high-charge
HCl	hydrochlorid acid
LB	Langmuir-Blodgett
LC	low-charge
LS	Langmuir-Schaefer
MFC	microfibrillar cellulose
NaCl	sodium chloride
$NaHCO_3$	sodium bicarbonate
NFC	nanofibrillar cellulose
NMMO	N-methylmorpholine-N-oxide
PAE	poly(amideamine) epichlorohydrin
PDADMAC	poly(diallyldimethylammonium chloride)
PEI	poly(ethylenimine)
PVA	poly(vinylalcohol)
PVAm	poly(vinylamine)
QCM-D	quartz crystal microbalance with dissipation
rms	root mean square
rpm	revolutions per minute
SPR	surface plasmon resonance
TEM	transmission electron microscopy
TFA	trifluoroacetic acid
TiO_2	titanium dioxide
TMSC	trimethylsilyl cellulose
TSC	thiosemicarbazone
XPS	X-ray photoelectron spectroscopy

TABLE OF CONTENTS

1 INTRODUCTION AND OUTLINE OF THE STUDY

Nanoscience is the emerging science which deals with the manipulation and characterisation of objects whose dimensions range from a few nanometers, i.e. the size of the largest molecules, to less than 100 nanometers. Nanotechnology is the engineering discipline that applies nanoscience to create products or processes based upon individual or multiple integrated nanoscale components (Ozin 2005, Whitesides 2005). During the past decade new technologies originating from nanoscience have emerged and opened opportunities in many fields, including forest products technology (Klemm et al. 2006, Hamad 2006). At the same time, the business environment of the traditional pulp and paper industry in the Nordic countries has been subject to change due to the transfer of production capacity to South America and Asia. This has been particularly challenging for the Nordic countries, where the forest industry has been one of the main industries for centuries. However, this changing environment is favourable for innovations, and hence, nanotechnology shows vast potential in finding new uses for cellulosic materials.

Cellulose is the main constituent in woody plants and the most renewable bioresource. In biosynthesis, cellulose polymers aggregate to form substructures, microfibrils, which in turn aggregate to form cellulosic fibres. Using new effective methods these fibrils can be disintegrated from the fibres to form uniform nanosized material. These nanofibrils have extremely good strength properties and potential in many nanotechnology applications, such as strength reinforcement in nanocomposites (Berglund 2005).

In this thesis work, properties and interfacial phenomena of cellulose nanofibrils were studied on a fundamental level in order to gain a deeper understanding of the behaviour of new nanofibril materials. More specifically, the aim was to characterise nanofibril materials, and to study the interactions of nanofibrils with water, polymers, and enzymes. The aim was also to find new applications for cellulose nanofibril materials in the forest products industry.

The overall goal of the projects "Nanostructured cellulose products" and "Designed cellulosic nanostructures" was to develop and characterise new nanofibrillar cellulose materials and to find new high-end applications for the materials. The projects were conducted in co-operation with STFI-Packforsk and the Royal University of Technology, KTH, Sweden, and the Department of Engineering Physics, TKK, Finland.

Preparation of cellulose nanofibrils using a novel pre-treatment procedure is presented in **Paper I**. The resulting material was thoroughly characterised with respect to dimensions and homogeneity of the material. Special attention was paid to the rheological properties of the aqueous cellulose nanofibril gels.

Complex materials provided by nature are a difficult subject of research due to difficulties in interpreting their behaviour, and also due to restrictions of analytical methods in surface science. Therefore, to fundamentally study the interactions of for example polymers or enzymes with cellulosic fibres, model systems are employed. The increased interest of using cellulose nanofibrils in nanotechnology also raised a need for a model surface prepared from the same material. Cellulose nanofibril model films were developed and characterised in the work reported in **Paper II**. The surfaces were found to be stable and suitable for quartz crystal microbalance with dissipation (QCM-D) studies and they were further utilised in preparing Papers III and V. The effect of fibril charge density, solution electrolyte concentration and pH on swelling and surface interactions of the model film was studied using QCM-D and atomic force microscopy (AFM) force measurements.

Several possible applications of cellulose nanofibrils include mixing cellulose with polymers. In the experiments reported in **Paper III** interactions between cellulose nanofibrils and different types of polymers were studied using QCM-D, surface plasmon resonance (SPR), and confocal laser scanning microscopy (CLSM). In the QCM-D measurements special attention was paid to the effect of polymer properties on the viscoelastic properties of the polymer/fibril interface. The dry mass of adsorbed polymers was determined by SPR. The effect of polymers on nanofibril aggregation was studied by confocal microscopy.

A paper chemical application of cellulose nanofibrils is presented in **Paper IV**. Cellulose nanofibrils were used as a strength-reinforcing agent together with a cationic polyelectrolyte, poly(amideamine) epichlorohydrin (PAE), to enhance the wet and dry strength of paper. The adsorption of nanofibrils and PAE on cellulose model surfaces was studied using quartz crystal microbalance with dissipation (QCM-D) and atomic force microscopy (AFM).

Properties of the cellulose nanofibril film were compared with properties of other cellulose model films. Special attention was paid to the effect of model film suprastructure and morphology on swelling and enzymatic hydrolysis of cellulose. Interaction of cellulose model surfaces with water was studied using QCM-D to see the effect of crystallinity on swelling properties (unpublished data, chapter 4.6.1). The interactions of cellulose nanofibrils with enzymes were studied in the work reported in **Paper V**. Cellulose nanofibril model films were used to study enzymatic hydrolysis upon incubation in cellulase enzyme mixtures using QCM-D and AFM imaging. The results on enzyme binding and substrate degradation were compared with three other types of models for cellulose.

2 BACKGROUND

2.1 Structure and chemistry of cellulosic fibres

The native cellulose molecule consists of linear glucan chains with repeating (1→4)-*β*-glucopyranose units. Cellobiose is the dimer of cellulose and it is the repeating unit of the polymer, as shown in Figure 1. The degree of polymerisation is determined by the number of single anhydroglucose units, and it varies depending on the origin of cellulose. Already 30 anhydroglucose units give the polymer the characteristic structure and properties of cellulose (Nehls et al. 1994) but the degree of polymerisation can be up to more than 15 000 monomers.

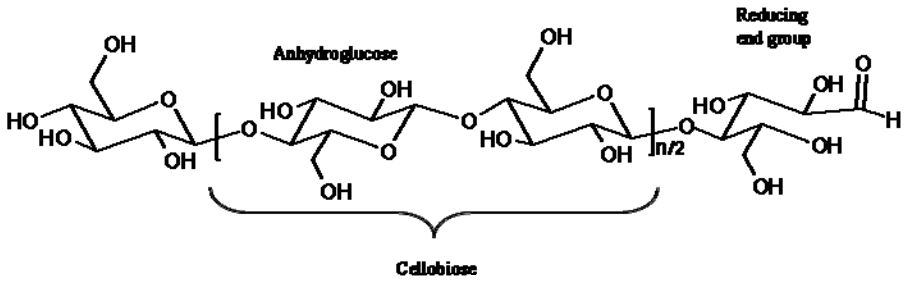

Figure 1. *Structure of cellulose (adapted from Kontturi et al. 2006).*

The supramolecular structure of cellulose is very complex and it has been the subject of debate for decades. Four different polymorphs of cellulose are known, cellulose I, II, III, and IV. In living plants cellulose occurs in fibres mostly in the crystalline form cellulose I and in less ordered amorphous regions (O'Sullivan 1997). Cellulose I has two allomorphs, I_α and I_β. These allomorphs differ in their hydrogen bonding patterns. I_α is a meta-stable phase with a triclinic unit cell containing one chain while I_β has two chains in its monoclinic unit cell. Cellulose II can be obtained from cellulose I by regeneration or mercerization. Regeneration involves solubilisation of cellulose I in a solvent followed by reprecipitation by dilution in water. Mercerisation is the process of swelling native fibres in concentrated sodium hydroxide followed by removal of the swelling agent. Cellulose I and II are the most studied forms of cellulose and their structural difference is highlighted in Figure 2. The dominant hydrogen bond for cellulose I is the O6-H---O3 whereas for cellulose II it is the O6-H---O2. Furthermore,

the chains in cellulose I run in parallel direction whereas cellulose II has an antiparallel packing.

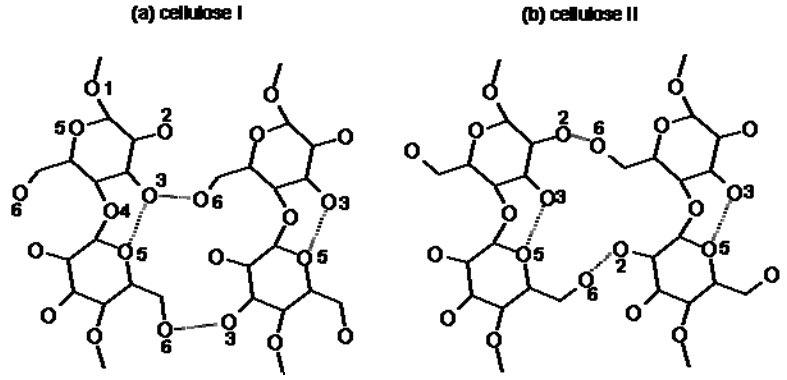

Figure 2. *Major supramolecular difference between (a) cellulose I and (b) cellulose II (adapted from Kontturi et al. 2006).*

Cellulose III_I and III_{II} are formed from celluloses I and II, respectively, by liquid ammonia treatment. Cellulose IV_I and IV_{II} are prepared by heating celluloses III_I and III_{II}, respectively. Cellulose III has a hexagonal unit cell while cellulose IV is reported to have an orthogonal unit cell (O'Sullivan 1997).

In the biosynthesis of wood, parallel synthesis of cellulose leads to noncovalent association of multiple chains, resulting in substructures termed microfibrils. These fibrils have high aspect ratio, and they consist of fully crystalline regions and amorphous less ordered regions. The smallest fibril unit is called elementary fibril which has been shown to be 2.5 - 4 nm in diameter (Jacob 1995, Hult 2001, Saito 2007) and up to a few micrometers in length. The elementary fibrils aggregate to form microfibrils which further aggregate into larger fibril bundles and finally cellulosic fibres, as shown in Figure 3.

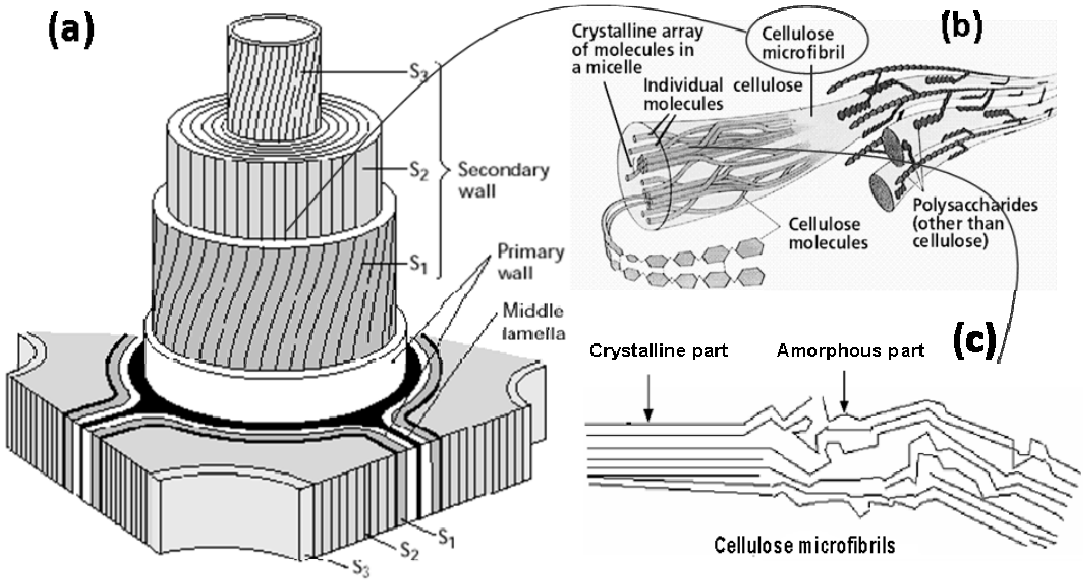

Figure 3. *(a) Composition of the wood cell wall (adapted from Taiz and Zeiger 2002). The cell wall is divided into primary and secondary walls, and the secondary wall further into S1, S2, and S3. (b) A schematic representation of cellulose microfibrils. (c) Schematics of a cellulose microfibril consisting of crystalline and amorphous regions.*

The cell wall of wood fibres consists of cellulose microfibrils which are surrounded by an amorphous matrix of hemicelluloses and lignin. The cell wall can be divided into several layers: a middle lamella, primary cell wall, secondary cell wall (S1, S2, S3) (Figure 3a), and warty layer. These layers differ from one another in terms of structure and chemical composition (Sjöstrom 1993). The middle lamella separates individual cells and it consists mainly of lignin. The primary wall consists mainly of amorphous hemicelluloses and lignin, but also some pectins, proteins and cellulose are present. The secondary wall is further divided into S1, S2, and S3 layers, and most of the cellulose is located in the secondary wall, especially in the thickest S2 layer. In each sublayer the cellulose chain axis is arranged in parallel to the axis of the microfibrils. Furthermore, the microfibril angle of the fibrillar network varies between the sublayers, being 50° to 70° for the S1 layer, 0° to 30° for the S2 layer, and 50° to 90° for the S3 layer, in relation to the fibre axis (Sjöström 1993). The warty layer is located in the inner surface of the cell wall in softwoods and in some hardwoods, and its chemical composition is still unknown.

2.2 Preparation and applications of nanostructured cellulose materials

A high aspect ratio and specific surface area combined with high strength and flexibility are characteristic for cellulose microfibrils. Functional hydroxyl groups in cellulose also enable chemical modifications for further applications. Biocompatibility, non-toxicity and biodegradability of cellulose nanomaterials are important properties in biochemical and biomedical applications. All these features make cellulose microfibrils a very promising material for nanotechnology. In this chapter the preparation, properties and applications of cellulose nanomaterials are described.

2.2.1 Fibrillar materials from wood pulp

In the beginning of the 1980s Turbak and co-workers (1983) introduced a method to disintegrate wood pulp fibres through a homogenisation process, resulting in liberation of microfibrils from the fibre matrix. This material was termed microfibrillated cellulose (MFC). The MFC material consisted of interconnected fibrils and microfibrils, which were 10-100 nm in width and formed a gel-like, highly viscous network already at low concentrations, i.e. 2% aqueous suspension (Turbak et al. 1983, Herrick et al. 1983). Major drawbacks of the procedure were the instability of the process due to clogging of the equipment and the high cost of the material due to the high energy consumption of the homogeniser. Mainly because of these drawbacks, the material was not further utilised despite the potential it had already shown for many applications (Turbak et al. 1983).

MFC was rediscovered at the turn of the 21st century, as nanoscience and nanotechnology started to attract researchers in the field of cellulose chemistry, and improved technologies for the disintegration process became available. Several groups have reported methods for preparing MFC similar to those introduced by Turbak et al. (Nakagaito and Yano 2004, Nakagaito and Yano 2005, Andresen et al. 2006, Andresen and Stenius 2007, Stenstad et al. 2008). These materials, however, are rather inhomogeneous and in addition to microfibrils, they contain larger fibril

bundles and residual fibre fragments. Effective grinders have also been used to produce MFC by introducing high shear stresses along wood fibres, but the resulting materials are also very inhomogeneous in size and the energy consumption of the grinders can be very high (Taniguchi and Okamura 1998, Iwamoto et al. 2005, Subramanian et al. 2008). Abe and co-workers (2007) presented a method to produce nanofibrillar cellulose by extracting wood powder to remove lignin and hemicelluloses, followed by disintegration of the remaining cellulose using a grinder. This material had a uniform width of 15 nm. The effect of hemicelluloses on fibrillation has also been studied by preparing never-dried and once-dried pulps from wood powder which were further disintegrated in a grinder (Iwamoto et al. 2008). The presence of hemicelluloses was found to facilitate fibre delamination, resulting in smaller and more uniform fibril dimensions.

Recently introduced novel disintegration methods combine either an enzymatic (Paper I) or a chemical pretreatment (Wågberg et al. 2008, Saito et al. 2007) of delignified pulp fibres with the mechanical disintegration process. Generally, the pretreatments promote the delamination process, resulting in lower energy consumption, better stability of the process, and smaller and more uniform dimensions of the fibrils. To distinguish between the different kinds of cellulose microfibril product introduced, these novel materials are here termed *cellulose nanofibrils* instead of microfibrils, a term which refers to the micrometer scale of the earlier materials. In this thesis, an enzymatic pre-treatment of delignified, high-hemicellulose-content softwood pulp fibres combined with mechanical refining prior to final disintegration in a high-pressure fluidizer is presented (Paper I). Wågberg et al. (2008) reported a chemical pre-treatment procedure in which delignified softwood pulp fibres were carboxymethylated prior to disintegration in a high-pressure fluidizer. Saito et al. (2007) presented an oxidation pretreatment method for hardwood pulp fibres. The fibres were oxidised by a 2,2,6,6,-tetramethylpiperidine-1-oxyl radical (TEMPO)-mediated system followed by very mild mechanical disintegration, i.e. agitation in water using magnetic stirrers (Saito et al. 2007). The chemical pre-treatment methods introduced by Wågberg at al. and Saito et al. both introduce anionic groups onto the fibril surfaces to promote fibre delamination, resulting in very homogeneous and highly anionic nanofibrils. Figure 4 shows a transmission electron microscopy (TEM) image of highly anionic nanocellulose material (Wågberg et al. 2008).

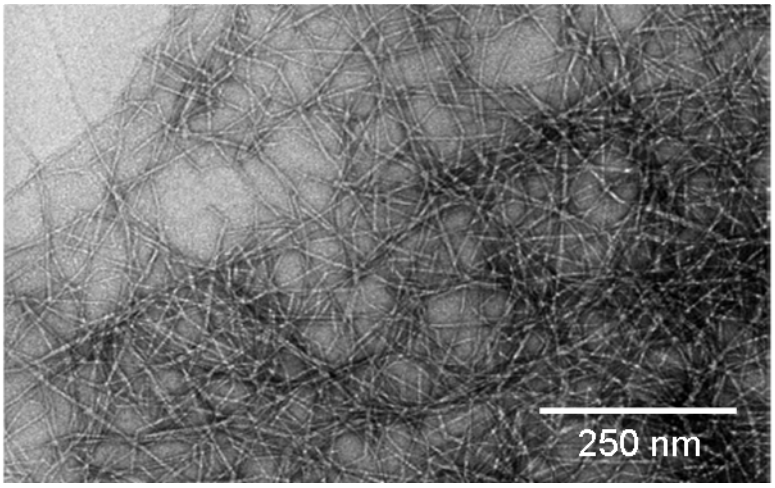

Figure 4. *TEM image of highly anionic cellulose nanofibrils. The nanofibril material was prepared by chemically pre-treating cellulosic fibres before disintegrating them in a homogenizer (adapted from Wågberg et al. 2008).*

The properties of cellulose micro- and nanofibrils differ greatly from the properties of wood pulp fibres mainly because of the large specific surface area and high aspect ratio of the fibrils. In aqueous suspensions the fibrils form a highly entangled network which behaves as a pseudoplastic gel (Herrick et al. 1983). The rheological properties enable the use of the fibril materials as thickeners or stabilisers in suspensions or emulsions (Andresen 2007a) in many applications such as foods, paints, cosmetics and pharmaceuticals (Turbak et al. 1983). The Young's modulus of cellulose fibrils has been reported to be 138 GPa and the extremely good strength properties and good thermal stability of the fibrils make them suitable for use as reinforcement in nanocomposites (Berglund 2005, Hubbe et al. 2008) and paper products (Turbak et al. 1983). Hydroxyl groups on cellulose fibril surfaces offer many possibilities for chemical modification, such as hydrophobization (Andresen et al. 2006, Lu et al. 2008), and these new functionalities can be utilised in further applications (Andresen and Stenius 2007). Homogeneous thin films of cellulose fibrils can be prepared upon drying and these films can be utilised for example in paper coatings. Films from hydrophobized fibrils can be used for water-repellent and self-cleaning material applications. Initially, cellulose microfibrils were proposed to be used in biomedical applications such as drug carriers (Turbak et al. 1983). Films from antimicrobial-grafted microfibrils have shown antibacterial behaviour, so the films could be used for example for wound healing or air filtration applications (Andresen et al. 2007). It is

noteworthy that although cellulose nanofibrils (and microfibrils) have potential in many applications, the number of established commercial products from nanofibrils is still very limited, but as the research in this area has expanded in the past few years, new commercial applications are expected to be launched in the near future.

2.2.2 Other nanocellulose materials

High-shear homogenization has also been applied to several other types of cellulose sources such as sugar beet, potato tuber and banana rachis. In these plants the microfibrils are easier to liberate from the fibre matrix than fibrils from wood, and the disintegration requires less energy. However, these materials are still somewhat heterogeneous and consist of large fibril bundles (Dinand et al. 1996, Dinand et al. 1999, Dufresne et al. 2000, Heux et al. 1999, Lowys et al. 2001, Zuluaga et al. 2007).

Cellulosic fibres can also be disintegrated into substructures by strong acid hydrolysis. In the acid hydrolysis the amorphous regions of cellulose microfibrils are attacked and the resulting material is crystalline, low-aspect-ratio cellulose (Rånby 1951, Battista et al. 1956, Marchessault et al. 1959, Marchessault et al. 1961, Revol et al. 1992, Revol et al. 1994, Dong et al. 1996, De Souza Lima et al. 2004). These rod-like crystallites are termed cellulose microcrystals or nanocrystals, depending on their size, but they are also referred to as whiskers or nanorods. Sulphuric acid has been widely used in the hydrolysis. This treatment results in particles which have anionic surface groups on the surfaces, leading to electrostatic stabilization of the particles in the suspension, see Figure 5a. The crystals have the ability to form chiral nematic liquid crystalline phases in concentrated solutions (Revol et al. 1992, Fleming et al. 2000, De Souza Lima et al. 2004). Possible applications of cast films include optically variable films and ink pigments for cosmetics and security papers (Fleming et al. 2001). Hydrochloric acid has also been used in the hydrolysis, leading to less stable suspensions due to smaller amounts of anionic groups on the crystal surfaces (Araki et al. 1998, Araki et al. 1999, Araki et al. 2000). The cellulose nanocrystals do not have the same gel-like properties as nanofibrils due to their rod-like shape, lower aspect ratio and crystalline suprastructure. However, because of the less elongated shape of the nanocrystals they are easier to use as reinforcement in composite materials (Berglund 2005, Hubbe et al. 2008). Other applications include pharmaceutical tablets

and food production additives, such as stabilizers, texturing agents and fat replacers (Fleming et al. 2001). In addition to wood fibres, cellulose nanocrystal suspensions have been prepared from many cellulose sources, namely, cotton (Revol et al. 1994, Dong et al. 1996, Dong et al. 1998), bacterial cellulose (Grunert and Winter 2002) and sea animals (Heux et al. 2000, Azizi Samir et al. 2004).

Bacterial cellulose (BC) is produced by *Acetobacter xylinum* and the material consists of long and individual cellulose fibrils, see Figure 5b. BC is a gel-like and very homogeneous material, and it is free of lignin, pectin and hemicelluloses. BC has been shown to be an interesting biomaterial, mainly because of its high purity and biocompatibility. BC has been used in several biomedical applications such as antimicrobial wound dressings, bone graft material, scaffold for tissue engineering of cartilage and blood vessels (Klemm et al. 2001, Svensson et al. 2005, Bodin et al. 2007a). Transparent polymeric nanocomposites have been prepared using BC as a reinforcing agent (Nogi et al. 2005). These nanocomposites are flexible, thermally stable and mechanically strong, and they can be used to prepare e.g. flexible displays in the electronics device industry (Nogi and Yano 2008).

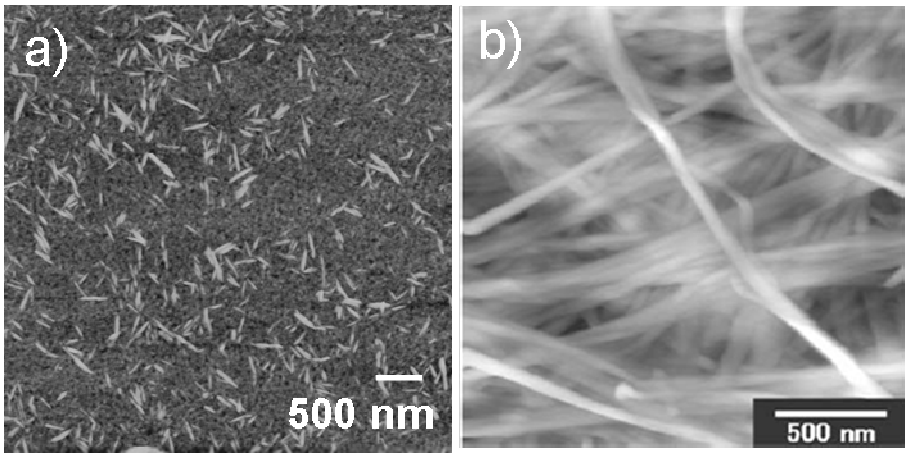

Figure 5. *AFM images of (a) cellulose nanocrystals (adapted from Kontturi et al. 2007) and (b) bacterial cellulose (adapted from Nakagaito et al. 2005).*

2.3 Cellulose model surfaces

Cellulosic fibres are complex composite structures. In addition, they are relatively small, rough, porous and heterogeneous. These features make cellulose a challenging subject of study. Therefore, to fundamentally study the interactions of cellulose with other matters, model systems are employed. Model surfaces enable fundamental studies of cellulose using interfacial methods such as atomic force microscopy (AFM), quartz crystal microbalance with dissipation (QCM-D), surface plasmon resonance (SPR) and ellipsometry. In this chapter, the preparation and applications of cellulose model surfaces are described.

2.3.1 Preparation of cellulose model surfaces

Cellulose model surfaces have been prepared using different approaches. The earliest cellulose model surfaces were reported by Luner and Sandell (1969), who prepared regenerated cellulose films from viscose and cellulose acetate. During the past 15 years, cellulose model surfaces have been extensively studied and developed (Kontturi et al. 2006). Langmuir-Blodgett (LB) deposition and spin coating are the most commonly used methods for preparing smooth cellulose model surfaces. Both methods involve dissolving or dispersing cellulose in a liquid before deposition on a solid substrate. Cellulose has been dissolved in solvents such as dimethylacetamide with lithium chloride (DMAc-LiCl), N-methylmorpholine-N-oxide (NMMO), or trifluoroacetic acid (TFA), (Schaub et al. 1993, Buchholz et al. 1996, Holmberg et al. 1997, Geffroy et al. 2000, Gunnars et al. 2002, Kontturi et al. 2003, Neuman et al. 2003), resulting in highly amorphous regenerated cellulose II films. Edgar and Gray (2003) introduced a method to prepare cellulose model surfaces by spin-coating cellulose nanocrystal suspensions, resulting in smooth and highly crystalline cellulose I surfaces. Cellulose I films have also been prepared by self-assembly of a cellulose (II) derivative, cellulose-thiosemicarbazone (TSC), on a gold substrate (Yokota et al. 2007). In this method the cellulose-TSC derivative was dissolved in NMMO and adsorbed on a gold-coated silicon substrate. Spontaneous reaction between the thiolated cellulose chains and the gold substrate resulted in reproduced cellulose I structure through self-assembly. Nanocrystalline cellulose I films have also been

prepared by Langmuir Blodgett deposition using cellulose nanocrystals hydrolyzed from ramie and tunicin fibres (Habibi et al. 2007). Recently, multilayer films of highly anionic cellulose nanofibrils and a cationic polymer, poly(ethyleneimine) (PEI), have been prepared by spin-coating (Aulin et al. 2008). These films consist of both crystalline cellulose I and amorphous less ordered regions. However, the cellulose material has been carboxymethylated prior to nanofibril preparation and hence the films do not represent the chemical structure of native cellulose.

2.3.2 Utilisation of cellulose model surfaces in interfacial science

Cellulose model surfaces have mainly been used to study fundamental aspects of adsorption and surface interactions, and the swelling of cellulose in aqueous media (Kontturi et al. 2006). Although the cellulose model surface research is mainly fundamental, many of the phenomena studied are linked to industrial problems in, for example, papermaking.

Cellulose model surfaces have been used to study adsorption of polymers, surfactants, and inorganic particles on cellulose using methods such as QCM-D, reflectometry, and ellipsometry (Kontturi et al. 2006 and the references therein, Tammelin et al. 2007, Aulin et al. 2008, Kontturi et al. 2008). Because of the great industrial importance of polyelectrolytes as a process and functional chemical in papermaking most of the adsorption studies have focused on the adsorption of polyelectrolytes on cellulose. Adsorption of surfactants on cellulose surfaces has also been studied because of their importance in papermaking where they are used as stabilizers and de-inking chemicals (Torn et al. 2005, Penfold et al. 2007).

An obvious application of smooth thin films of cellulose is surface force studies (Kontturi et al. 2006 and the references therein, Stiernstedt et al. 2006, Notley et al. 2006, Salmi et al. 2007). For example, the fibre-fibre interactions involved in the formation of fibre-fibre bonds, which constitute the basis of the paper web, have been studied by force measurements. In addition, surface interactions between cellulose and polymers, minerals and peptides have been studied. Other applications of cellulose model surfaces in force measurements include friction force and adhesion measurements (Stiernstedt et al. 2006).

Cellulose model surfaces have also been used as moisture sensors to examine the swelling of cellulose in aqueous media which is of great interest in many industrial applications of cellulosic fibres (Kontturi et al. 2006). In addition, cellulose model surfaces have been used to study wetting kinetics of cellulose. Another popular subject of research has lately been enzymatic hydrolysis of cellulose, for example to produce energy from cellulose. QCM has been used to study the binding of enzymes on cellulose model surfaces and also to monitor the cellulose degradation kinetics and changes in cellulose film properties during the hydrolysis (Eriksson et al. 2005, Josefsson et al. 2008, Turon et al. 2008, Rojas et al. 2007).

In this thesis work, cellulose nanofibril model films were developed and utilised to study the swelling of a cellulose nanofibril network in aqueous conditions and to study the surface interactions of nanofibrils in varying conditions. Polymer adsorption on nanofibrils and enzymatic hydrolysis of nanofibril films were also studied. The cellulose material used for film preparation was chemically unmodified nanofibril material from wood pulp and hence these novel cellulose model films were representative models for native cellulosic fibres. In addition, different types of cellulose model surfaces were used to compare the effect of cellulose suprastructure, chemistry, and model film morphology on swelling and enzymatic hydrolysis. Further characterisation of cellulose model surfaces was done by measuring model film crystallinity.

3 EXPERIMENTAL

The materials and methods used in the experiments included in this thesis are described in detail in the attached Papers I-V. Thus, this chapter gives a more general overview of the experimental design and provides some background on the methods used.

3.1 Materials

3.1.1 Nanofibril materials

The nanofibril materials used were disintegrated from bleached softwood sulphite pulp by using a high-pressure fluidizer (Microfluidizer M-110EH, Microfluidics Corp., Newton, MA) at STFI-Packforsk, Stockholm, Sweden. Two different types of nanofibril materials, low-charge (LC) and high-charge (HC), were used. The hemicellulose contents of the reference pulps were 13.8% and 4.5%, respectively, constituting mainly of xylan and glucomannan. The LC nanofibrils were pre-treated with enzymatic hydrolysis and mechanical refining before disintegration of the fibres in the high-pressure homogenizer. The preparation of the LC fibrils is described in detail in Paper I. The HC nanofibrils were prepared by performing a carboxymethylation pre-treatment for the pulp before the homogenization process (Wågberg et al. 2008). This pre-treatment resulted in an increased amount of anionic carboxyl groups on the fibrils, giving the material higher surface charge. In addition, the carboxymethylation made the fibres easier to delaminate, resulting in lower energy consumption and smaller dimensions of the nanofibrils compared to the enzymatic pre-treatment. Full disintegration was achieved with a single pass through the homogenizer (Wågberg et al. 2008) in contrast to 8 passes that were required in case of the enzymatic pre-treatment (Paper I).

In order to prepare transparent, stable dispersions from the 2% nanofibril gels for model surface preparation (Papers II-IV) and adsorption experiments (Paper V), the gels were diluted with Milli-Q water to 1.67 g/L, stirred with an ultrasound microtip for 10 min at 25% amplitude setting, and centrifuged in an Optima L-90K

ultracentrifuge from Beckman Coulter, USA at 10400 rpm (10000 G) to remove remaining fibril aggregates. The centrifugation time was 45 min and 2 h for LC and HC nanofibrils, respectively, and the corresponding concentration of the fibrils in the supernatant was approximately 0.4 g/L and 1.2 g/L. This indicates that 24% of the LC nanofibril sample and 72% of the HC nanofibril sample remained in the supernatant.

3.1.2 Other cellulose materials for model surfaces

Trimethylsilyl cellulose (TMSC) was prepared by silylation of microcrystalline cellulose powder from spruce with hexamethyl disilazane according to Greber and Paschinger (1981) and Cooper at al. (1981). The synthesis details have been reported in detail by Tammelin et al. (2006). TMSC conversion to cellulose by desilylation was carried out according to Schaub et al. (1993).

Cellulose was dissolved in dimethylacetamide/lithium chloride (DMAc-LiCl) in order to prepare amorphous cellulose films in the experiments in chapter 4.6.1. The cellulose dissolution was performed according to Berthold et al. (2004) without the derivatizing agent. Cellulose was dissolved in N-methylmorpholine-N-oxide (NMMO) in order to prepare regenerated cellulose surfaces according to Gunnars et al. (2002). Dissolving pulp (Domsjö fabriker, Sweden) and micro-crystalline cellulose (Avicel) were dissolved in NMMO in experiments described in chapter 4.6.1 and Paper V, respectively.

Cellulose nanocrystals were prepared in two different ways. In the experiments in chapter 4.6.1 a colloidal suspension of cellulose nanocrystals was prepared by sulphuric acid hydrolysis of a dissolving-grade pulp according to Dong et al (1996). In the experiments in Paper V, the cellulose nanocrystals were obtained by HCl acid hydrolysis of Whatman cellulose filter paper (Kim et al. 2006), followed by grinding in a blender.

3.1.3 Substrates and anchoring substances

Several different types of cellulose model surface were studied and prepared in this thesis. The model surfaces were prepared in collaboration with two other research

groups, which led to the use of several different substrates, washing procedures, and differences in the final film formation.

Substrates used for nanofibril film preparation were silica QCM crystals (Q-Sense AB, Västra Frölunda, Sweden) or smooth silica wafers (Okmetic Oy, Helsinki, Finland and MEMC Electronic Materials SpA, Novara, Italy). In the experiments reported in Paper II, a series of anchoring substances were tested to improve the coverage of LC nanofibrils on a silica substrate. 3-aminopropyltrimethoxysilane (APTS) was shown to be the most efficient anchor for the LC nanofibrils and was hence used as the anchoring substance for the LC nanofibril film in the experiments reported in Papers II-IV. For the SPR measurements reported in Paper III cellulose nanofibril films were prepared on PVAm-coated gold substrates

In the experiments reported in chapter 4.6.1 poly(ethyleneimine) (PEI) was adsorbed on silica substrates as an anchoring polymer for regenerated DMAc-LiCl and NMMO cellulose, HC nanofibrils, and cellulose nanocrystals. In Paper V, regenerated NMMO cellulose surfaces were prepared on washed gold QCM-crystals and poly(vinylamine) (PVAm) was used as an anchoring polymer.

Substrates used for Langmuir-Schaefer film preparation were QCM-D crystals which were spin-coated with polystyrene by the supplier. For the crystallinity measurements described in chapter 4.6.1 the LS cellulose films were prepared on hydrophobized silica wafers.

3.1.4 Enzymes, polymers, and other chemicals

The enzyme used in the experiments described in Paper V was a commercial mixture (NS50013 cellulase complex, Celluclast) from Novozymes, which is an aqueous solution (700 U/g and an activity of 68 FPU/g). The enzyme mixture is obtained from *Trichoderma reesei* fungus and it contains endoglucanases, cellobiohydrolases, and β-glucosidases. Sodium acetate buffer solutions (pH 5) were used in the hydrolysis.

Polymers used for the adsorption experiments reported in Paper III were poly(diallyldimethylammonium chloride) (PDADMAC), xyloglucan, and

carboxymethyl cellulose (CMC). PDADMAC (Allied Colloids Ltd) was ultrafractioned with an Amicon ultrafiltration unit using a cutoff >300 000. Tamarind xyloglucan (Megazyme) and CMC (Finnfix WRM) were used as delivered.

In the work described in Paper IV the cationic polyelectrolyte used was a commercial sample of poly(amideamine) epichlorohydrin (PAE) (Wetres PA 13, Kemira Oyj, Finland). The solution was used as delivered.

All other chemicals were of analytical grade if not otherwise specified.

3.1.5 Pulp

The pulp used for preparing the paper hand sheets for the experiments reported in Paper IV was a bleached pine kraft pulp from Metsä-Botnia, Finland. Before use, the pulp was refined according to SCAN 25:76 for 5 min to fibrillate the fibre surfaces. The fines material was removed from the pulp using a 80-mesh wire. Finally, the pulp was washed to its sodium-form prior to hand sheet preparation (Swerin and Wågberg 1994).

3.2 Methods

The main experimental methods used in this thesis were QCM-D and AFM imaging. In addition, cellulose model film preparation was used and the films were mainly prepared with the spin-coating technique. The principles of these methods are presented here in more detail. For details of the other methods used the reader is referred to Papers I-V and the references presented in this chapter.

3.2.1 Model film preparation

Spin-coating. In the spin coating technique a film is deposited on a solid surface from a volatile solvent by spinning the substrate at high speed (Larson and Rehg 1997, Norrman et al. 2005). The substrate is attached to a chuck which is spun at a desired rate. The thickness and roughness of the formed film can be controlled by varying

selected parameters. The main adjustable parameters in the spin coating equipment are spinning velocity, acceleration and the time of spinning. The solution's concentration and solvent properties also affect the film properties. In this thesis work cellulose model surfaces were prepared on QCM crystals and silica wafers with the spin coating technique, as presented in Figure 6. Aqueous cellulose dispersions (nanofibrils and nanocrystals), cellulose solutions (NMMO and DMAc-LiCl) or cellulose derivative solutions (TMSC) were used.

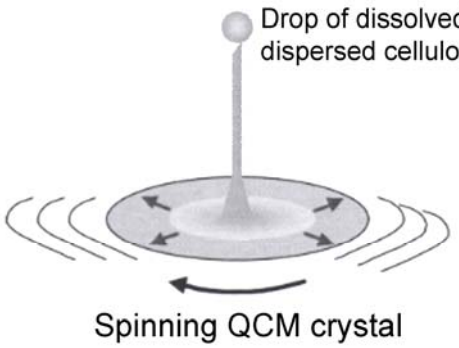

Figure 6. Illustration of a spin coating setup for preparing cellulose films (adapted from Enarsson 2008).

In the Langmuir-Blodgett (LB) technique a monolayer of water-insoluble compounds is made at a water/air interface (Langmuir 1917, Blodgett 1935). This monolayer can be further transferred onto a solid substrate. TMSC was used as an insoluble component which was dissolved in a volatile solvent (chloroform). In this work a horizontal dipping procedure was used because of limitations originating from the structure of the QCM-D crystals (Langmuir and Schaefer 1938). This procedure is called the Langmuir-Schafer (LS) method and the preparation of the LS cellulose surfaces on QCM crystals is reported in detail in Tammelin et al. (2006).

3.2.2 Quartz Crystal Microbalance with Dissipation (QCM-D)

Swelling, enzymatic degradation and adsorption of polymers on cellulose model surfaces were studied using the quartz crystal microbalance with dissipation (QCM-D). The QCM-D measures simultaneously changes in frequency and dissipation (frictional losses due to viscoelastic properties of the adsorbed layer) at the fundamental resonance frequency and its overtones (Rodahl et al. 1995). Figure 7 shows a schematic of the QCM-D technique.

Without adsorbate the crystal oscillates at a resonant frequency f_0 and upon adsorption the resonance frequency decreases to f. For uniform, rigidly adsorbed films the change in frequency, Δf, is proportional to the adsorbed mass per unit surface, Δm, according to the Sauerbrey equation (Sauerbrey 1959, Höök et al. 1998):

$$\Delta m = -\frac{C\Delta f}{n} \qquad (1)$$

where n is the overtone number and C is a device sensitivity constant. The relation is valid when the adsorbed mass is small compared to the mass of the crystal.

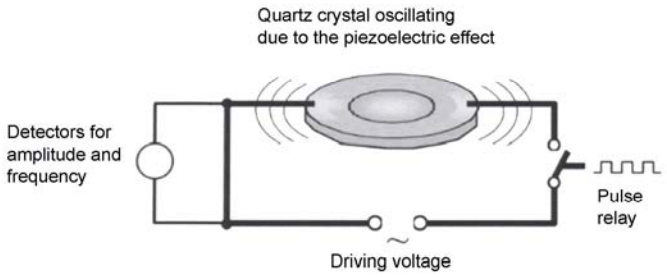

Figure 7. *Working principle of QCM-D. A quartz crystal vibrates at its resonant frequency, driven by a pulsed sinusoidal voltage. Changes in frequency are detected upon adsorption of particles (adapted from Enarsson 2008).*

The dissipation measurements in QCM-D give information about the viscoelastic properties of the adsorbed layer. When the voltage applied to the QCM-D is cut off

the amplitude decays due to frictional losses in the system. The decay rate depends on the viscoelastic properties of the adsorbed layer, the surrounding solution and the crystal itself. The change in the dissipation factor, $\Delta D = D\text{-}D_0$, can be measured as a function of time. D_0 is the dissipation factor of the crystal in solution and D is the dissipation factor after material has been adsorbed on the crystal. The dissipation factor D is defined by

$$D = \frac{E_{diss}}{2\pi E_{stored}} \qquad (2)$$

where E_{diss} is the energy dissipated during one oscillation and E_{stored} is the total energy stored in the oscillating system. A rigid adsorbed layer gives no change in the dissipation energy but for loose, viscoelastic adsorbing layers there is an increase in dissipated energy as a function of adsorption. In this thesis work the energy dissipation data were utilised to make interpretations of the viscoelasticity of adsorbed polymer layers on cellulose and also to study the viscoelastic changes upon swelling of cellulose model films in aqueous solutions. In addition, changes in cellulose model film structure and viscoelasticity upon enzymatic hydrolysis of cellulose was studied.

For ultrathin rigid films the changes in the frequency and the damping constants depend only on the mass of the films. However, thicker films show pronounced viscoelastic effects, and the Sauerbrey equation is no longer valid, and it tends to underestimate the amount of the adsorbed mass. Johannsmann et al. (1992) presented a model which allows calculation of the true sensed mass for viscoelastic layers

$$\delta\hat{f} \approx -f_0 \frac{1}{\pi\sqrt{\rho_q \mu_q}} \left(f\rho d + \hat{J}(f)\frac{f^3 \rho^2 d^3}{3} \right) \qquad (3)$$

where $\delta\hat{f}$ is the shift in frequency, f_0 is the fundamental frequency for the crystal in air, f is the resonant frequency of the crystal in contact with solution, d is the thickness of the film, and $\hat{J}(f)$ is the shear compliance. The quantities ρ_q and μ_q are the specific density and elastic shear modulus for quartz, respectively. ρ is the density of the fluid.

Equation 3 can be cast into a more convenient form by introducing the equivalent mass m^* defined by

$$\hat{m}^* = -\frac{\sqrt{\rho_q \mu_q}}{2f_0}\frac{\delta\hat{f}}{f} \qquad (4)$$

From Equation (4) one thus obtains

$$\hat{m}^* = m^0\left(1 + \hat{J}(f)\frac{\rho f^2 d^2}{3}\right) \qquad (5)$$

The true sensed mass (m^0) can be calculated by assuming that $\hat{J}(f)$ is independent of the frequency in the accessible frequency range. By plotting the equivalent mass against the square of the resonance frequency (f^2), the true sensed mass is given as the intercept (Naderi and Claesson 2006). In this thesis Johannsmann's model was used in the work reported in chapter 4.6.1 to calculate the amount of adsorbed water in swollen cellulose model films.

QCM-D experiments. In this thesis work, the experiments were performed using the Q-Sense E4-instrument from Q-sense, Västra Frölunda, Sweden, which is designed for controlled flow measurements. Sample liquids were pumped through the measurement chambers with a peristaltic pump at a rate of 0.1 mL/min. The changes in frequency and dissipation were followed as a function of time at 5 MHz and its overtones (15, 25, 35, 45, 55, and 65 MHz).

3.2.3 Atomic Force Microscopy (AFM)

AFM imaging. AFM imaging was used to characterise the dimensions and homogeneity of cellulose nanofibril products and to characterise changes in cellulose model surface structure and morphology before and after polymer adsorption or enzymatic hydrolysis. Developed in the mid-1980s (Binnig et al. 1986), AFM is an area of scanning force microscopy (SFM). Since then, AFM has become one of the most successful instruments in surface science. The AFM apparatus consists of a

sharp tip attached to a cantilever. The tip scans in the near field of the surface of the sample studied and the interactions between the surface and the tip are recorded. When a laser beam is directed to the cantilever, the deflection of the cantilever can be detected from the beam with a photo detector. AFM has different operating modes, namely, contact and dynamic modes. The dynamic mode is further divided into intermittent contact (tapping) and non-contact modes. In the contact mode the AFM tip scans the surface in contact with the surface. In the dynamic mode the cantilever is vibrating at or near its resonance frequency and measuring the changes in amplitude or frequency near the sample. In this thesis work, the tapping mode was used and it is hence discussed here in more detail.

In tapping mode the oscillation frequency is constant and the changes in amplitude are monitored (Zhong et al. 1993). During each oscillation cycle the tip is briefly in contact with the surface and the interaction forces between the sample and the tip cause a reduction in amplitude. The force applied to the surface is varied by changing the free amplitude of oscillation (A_0) and the set-point amplitude (A_{sp}). The set-point amplitude is the amplitude when the tip is in contact with the sample, showing the allowed damping of the signal. During the measurement, the A_{sp} is kept constant by moving the sample up and down. The topography (height) image is generated from the movement of the scanner. In addition to the amplitude changes, the cantilever motion can be characterised by its phase relative to the driving oscillator. The phase signal changes when the tip encounters regions of different composition. The cantilever loses energy due to the viscous damping of the medium and due to the tip-sample interaction. The vibrational characteristics of the cantilever can be described using the harmonic approximation

$$A(t) = A_0 \cos(\omega t + \delta)) \qquad (6)$$

where A_0 is the maximum amplitude during the oscillation cycle, $\omega=2\pi f$, f is the oscillation frequency, t is time and δ is the phase shift angle. The phase shift angle between the tip and the driving force is initially set to 90^o. When the tip approaches the sample, the amplitude decreases and the standing wave of the harmonic motion is affected. When the sample is scanned with the tip, the phase angle changes are

recorded and a phase shift image is achieved. AFM phase imaging detects variations in chemical composition, adhesion, friction and viscoelasticity in the sample surface.

In this work a Nanoscope IIIa Multimode scanning probe microscope from Digital Instruments Inc., Santa Barbara, CA, USA was used. The images were scanned in tapping mode in air using silicon cantilevers (NSC15/AIBS from MicroMash, Estonia) and the drive frequency of the cantilever was about 300-330 kHz. The size of the images scanned varied from 1 μm × 1 μm to 5 μm × 5 μm. No image processing except flattening was made.

AFM colloidal probe technique. The AFM was initially designed as an imaging tool but the possibility to measure surface forces was soon realised (Ducker et al. 1991). If commercial AFM imaging tips are used for measuring surface forces, the exact geometry of the tip is unknown, which complicates analysis of the force-distance curves. To overcome this problem, probes with well-defined geometry can be attached onto the cantilever. In addition, the probe also allows measurement of the material of interest. This technique is known as the colloidal probe technique (Butt 1991, Ducker et al. 1991). The colloidal probe technique is a method for characterising interfacial phenomena by measuring forces as a function of distances between surfaces. In this thesis work, the colloidal probe technique was used in the experiments reported in Paper II to study the interaction of the nanofibril model surfaces and a cellulose sphere in varying aqueous conditions. For further details of the principles of the method the reader is referred to Butt et al. (2005).

3.2.4 Other analyses

Transmission Electron Microscopy (TEM). Cellulose nanofibril dimensions and homogeneity were characterised using TEM (Paper I). A Tecnai 12 transmission electron microscope with Gatan 910 cryotransfer was used. The cryo-TEM method has been described in more detail by (Williams and Carter 1996).

Dynamic rheology. Nanofibril gel rheology was studied with a controlled strain rheometer (AR 2000, TA Instruments) using cone-and-plate and plate-and-plate

geometries in the work reported in Paper I. The theory and interpretation of the rheology measurements are described in more detail in (Barnes et al. 1989).

X-ray Photoelectron Spectroscopy (XPS). The coverage and chemical composition of cellulose nanofibrils (Paper II), and the nitrogen content of the adsorbed PAE-nanofibril layers (Paper VI) were determined using XPS. For further details of the interpretation of the XPS data, see ref. (Briggs and Seah 1992). In this work, a Kratos Analytical AXIS 165 electron spectrometer with a monochromated A1 Kα X-ray source was used.

Ellipsometry. Ellipsometry was used in the work described in Chapter 4.6.1 to determine the thickness of cellulose model surfaces by using a manual nulling photoelectric ellipsometer with a mercury lamp (5461 nm) (Type 43702-200E, Rudolph Research, Fairfield, USA). The azimuths delta (Δ) and psi (ψ) values were collected and the cellulose film thicknesses were determined by fitting the measured data to a three-layer model. At least three points were measured for each substrate studied to obtain an average film thickness and to determine the film homogeneity. The theory and interpretation of the ellipsometry measurements are described in more detail in (McCrackin et al. 1963).

Small Angle Incidence X-ray Diffraction. Crystallinity of the cellulose model films was determined using small angle incidence X-ray diffraction in the work reported in chapter 4.6.1 (unpublished data). The measurements were performed in the Department of Chemical Science and Engineering at Kobe University, Japan. Monochromatic synchrotron radiation, generated on a beamline BL-46 XU at a Super Photon ring 8 GeV (Spring-8, Nishi Harima, Hyogo, Japan), was irradiated onto the cellulose model films using small angle incidence geometry. The diffraction profiles were curve-resolved into noncrystalline scattering and crystalline reflections using a Rigaku multi-peaks separation software. The apparent crystallinity was evaluated from the area ratio. In order to check reproducibility, same measurements were performed for several samples using a laboratory scale rotating anode type X-ray diffraction apparatus (Mac Science, Ltd., Sra-Ml8X) combined with a Ge (111) incident monochromator and a goniometer with a thin film attachment.

Surface Plasmon Resonance (SPR). SPR was used in the work reported in Paper III to study the adsorption of polymers on cellulose nanofibril model surfaces. The adsorption of polymers was measured using a Biacore 1000 instrument (GE Healthcare, Sweden). The dry mass of adsorbed polymers was calculated based on the SPR results and compared to QCM-D results which give the combined amount of the adsorbed polymer and water that binds on the surface. The SPR technique has been described in more detail by Schasfoort and Tudos (2008).

Confocal Laser Scanning Microscopy (CLSM). The effect of polymer adsorption on cellulose nanofibril aggregation was verified using confocal microscopy in the work reported in Paper III. Confocal images were recorded with a Zeiss LSM 5 Duo laser-scanning confocal microscope (Carl Zeiss, Germany).

3.2.5 Paper hand sheet preparation and testing

In the experiments reported in Paper IV the paper hand sheets were prepared according to the standard SCAN-C 26:76. After drum drying the sheets were cured in an oven at 105 ^{o}C for 10 min. The wet and tensile strengths of the sheets were determined according to the standards SCAN-P 20:95 and SCAN-P 67:93, respectively. The attached amount of PAE in the hand sheets was determined by measuring the bulk nitrogen content of paper using the Antek 7000 chemiluminiscence equipment.

4 RESULTS AND DISCUSSION

This chapter summarises the most important findings of this work. The more detailed results can be found in the attached Papers I-V.

4.1 Preparation and characterisation of cellulose nanofibrils

The preparation and characterisation of cellulose nanofibrils, which constituted the basis for this thesis work, was done in collaboration with several research groups (see chapter 1 and Paper I). The characterisation of the material was of great importance to determine the quality of the novel nanomaterials produced but also to learn about the material properties, because nanocellulose materials differ significantly from cellulosic fibres.

Cellulose nanofibrils were prepared by combining an enzymatic pre-treatment of delignified, high-hemicellulose-content softwood pulp fibres with mechanical refining prior to final disintegration in a high-pressure fluidizer (Paper I). Monocomponent endoglucanases were used to selectively hydrolyze noncrystalline cellulose regions, allowing mechanical disintegration of fibres into high-aspect-ratio nanofibrils. The high hemicellulose content of the pulp fibres decreased the cell wall cohesion of the fibres, promoting cell wall delamination and decreasing the energy consumption compared with the preparation of earlier microfibrillar cellulose materials (Turbak et al. 1983). In addition, the enzymatic pre-treatment prevented clogging of the homogenizer which had limited the disintegration efficiency in previous attempts.

The dimensions and homogeneity of the cellulose nanofibril material were studied using TEM and AFM. Both microscopy measurements revealed that the fibrils have a high aspect ratio and that they form entangled network structures with other fibrils, as shown in Figures 8 and 9. The microscopy measurements showed that the material consists mainly of individual fibrils, though there are also some larger fibril bundles and fibril aggregates present in the material. The length of the fibrils was difficult to determine due to the above-mentioned entangled network structure, but the fibril length was estimated to be up to several micrometers. The width of the fibrils,

determined from the TEM images, was about 5 nm, see Figure 8. Similar nanofibril dimensions have been obtained by combining chemical pre-treatments with disintegration of pulp fibres (Wågberg et al. 2008, Saito et al. 2007).

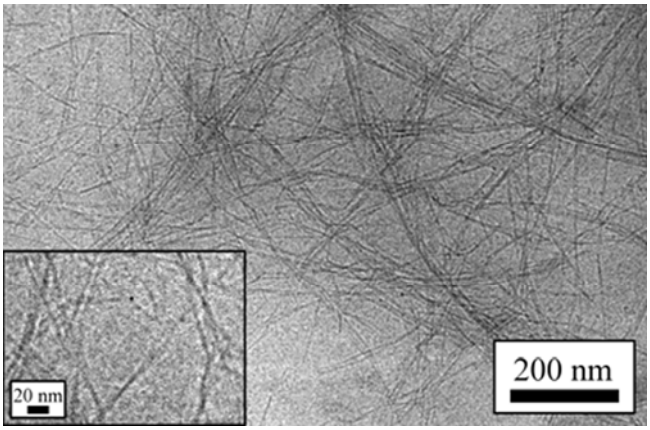

Figure 8. *Cryo-TEM image of cellulose nanofibrils prepared by combined enzymatic and mechanical treatments (Paper I).*

AFM imaging (Figure 9) showed a width of about 20-30 nm which is larger than what was observed with TEM. The larger width of the fibrils can be due to the drying of fibrils or fibril aggregates which affects the dimensions because aggregation or flattening may occur. In addition, the actual size of the AFM tip used introduces a small error in the measured diameters of the fibrils. The height of the fibrils was determined to be about 5 nm, which correlates with the TEM measurements.

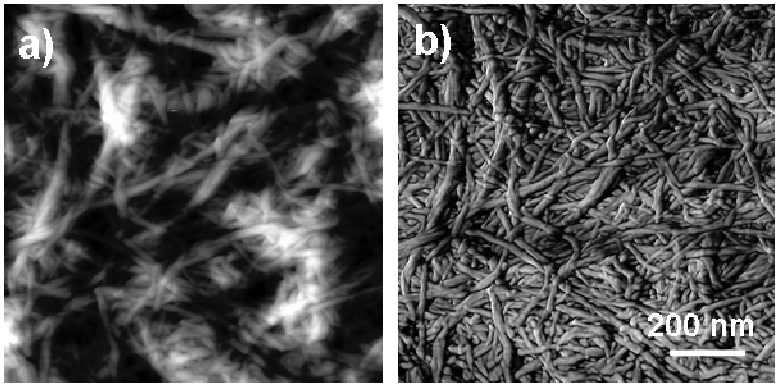

Figure 9. *a) Height, and b) phase contrast AFM images of cellulose nanofibrils prepared by combined enzymatic and mechanical treatments. The scan size is 1 μm ×1 μm and the data range is 50 nm.*

The network structure and high water retention capacity are characteristic of fibrillar cellulose materials (Herrick et al. 1983). The fibrils form gels already at low concentrations, which is a feature that affects all the possible applications of the material. Thus, it was of great interest to study the rheological properties of the nanofibril gels. The dynamic rheology investigations reported in Paper I (see Figure 10) revealed a gel-like behaviour for all the nanofibril concentrations (0.125%-5.9% w/w) used, with the storage modulus G' ranging from 1.5 Pa to 10^5 Pa. Thus, the modulus of the gel can be tuned 5 orders of magnitude by raising the concentration from about 0.1% to 6%. All the suspensions showed a large decrease in viscosity with increasing shear rate i.e. shear thinning, as was recognised at an early stage by Herrick et al. (1983). The maximum storage modulus was very high, i.e. about two orders of magnitude larger than typically observed for non-entangled low-aspect-ratio cellulose I gels (Ono et al. 2004, Tatsumi et al. 2002, Rudraraju and Wyandt 2005a, 2005b). This is due to the high aspect ratio of the nanofibrils, which leads to drastically enhanced strength of the gel network.

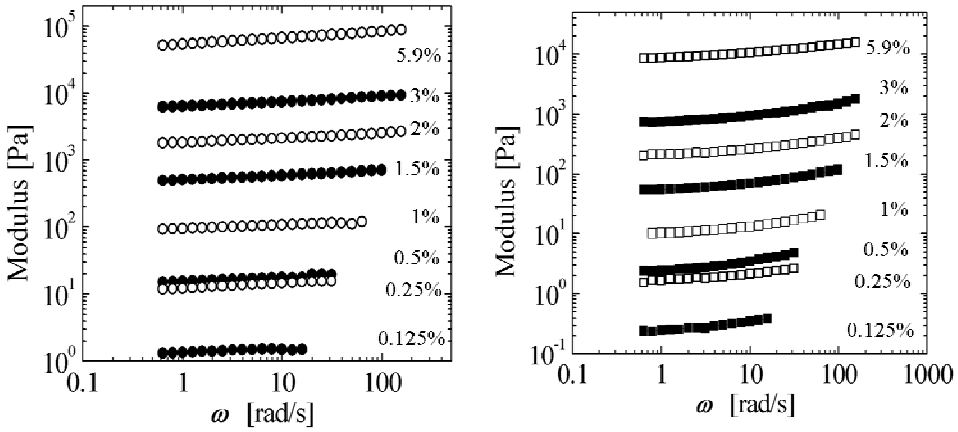

Figure 10. *Storage modulus G' (left) and loss modulus G'' (right) as a function of frequency for nanofibril suspensions (Paper I). Geometries used were steel plate for 5.9%, aluminium cone-and-plate for 1%-3% and acrylic plate for 0.125%-0.5% nanofibril suspensions.*

The dimensional characterisation and rheology results indicated that the enzymatic pre-treatment, combined with mechanical shearing prior to final homogenization, produces nanoscale high-aspect-ratio fibrils which form entangled strong network structures. Chemical fibre pre-treatments, which produce highly anionic nanofibrils, have also been shown to result in similar fibril properties (Wågberg et al. 2008, Saito et al. 2007). These properties can be utilised in new applications in materials science, for example, as reinforcement in nanocomposites.

4.2 Development of nanofibril model surfaces

Development of the nanofibril model surface (Paper II) constituted the groundwork for the fundamental interaction studies in this thesis. The model surface enabled the use of e.g. QCM-D and AFM to study the interactions of nanofibrils with water, enzymes and polymers. The nanofibril model surfaces were further utilised in the work reported in Papers II, III and V.

4.2.1 Preparation of the model surfaces

Preparing a stable aqueous dispersion from the nanofibril gels enabled the use of the spin-coating technique for film preparation. Ultrasound treatment combined with ultracentrifugation was shown to be an effective procedure for dispersing the entangled fibrils and removing remaining fibril aggregates (see Chapter 3.1.1). Two different types of cellulose nanofibril were used to prepare model surfaces. Low-charge (LC) nanofibrils were prepared with combined enzymatic and mechanical pre-treatment followed by homogenization. High-charge (HC) nanofibrils were prepared by carboxymethylating the pulp fibres before disintegration, which led to a higher total charge of the nanofibrils. In preliminary experiments the LC nanofibrils did not form a fully covered film on the silica substrate and hence a series of anchoring substances were used to improve the coverage. Poly(vinylamine) (PVAm), poly(vinylalcohol) (PVA), poly(ethyleneimine) (PEI), TiO_2, regenerated cellulose (TMSC), and 3-aminopropyltrimethoxysilane (APTS) were coated on silica crystals followed by spin-coating of the LC nanofibril dispersion. AFM imaging was performed to characterise the coverage of the surfaces. AFM imaging revealed that APTS gives the best coverage of the LC nanofibrils (Paper II). APTS was hence used as the anchoring substance for the LC nanofibril film in the work reported in Papers II, III and V.

HC nanofibrils were spin-coated directly onto bare silica surfaces and, surprisingly, no anchoring substances were needed. This can be due to the carboxyl groups in the HC nanofibrils which decrease the interactions between the fibrils and results in increased interactions between the fibrils and the substrate. The interaction between the HC fibrils and silica is suggested to be due to hydrogen bonding between hydroxyl groups on the silica substrate and cellulose. Because of the nature of the interaction, heat-treatment of the films was required to keep the films stable in aqueous conditions (Edgar and Gray 2003). The mechanism behind the heat treatment is believed to be strengthening of the bonding due to removal of water from the film. The water molecules no longer act as mediators between cellulose and silica i.e. the hydrogen bonding occurs directly between the cellulose fibrils and the silica surface. To determine possible dimensional changes due to the heat treatment, AFM imaging of the films was performed before and after the heat treatment. The images did not show

significant dimensional changes and images taken before the heat treatment are hence not shown.

4.2.2 Characterisation of the model surfaces

AFM imaging was used to characterise the nanofibril model surfaces in terms of surface morphology, roughness and thickness. Figure 11 shows AFM height images of the LC (a, b) and HC (c, d) nanofibril films. The LC nanofibril film shows a fibrillar network structure with an average rms roughness of 4 nm (over an area of 25 μm^2), whereas the HC film shows a denser and smoother film structure with an average rms roughness of 2 nm. It is also evident from the images that the HC fibrils have smaller and more uniform dimensions compared to the LC fibrils. This is due to the carboxymethylation pre-treatment which makes the pulp fibres easier to delaminate compared to the enzymatic pre-treatment. In addition, the anionic charges stabilize the fibril suspension electrostatically and thus prevent re-aggregation of the nanofibrils. The dimensional difference was also observed as a higher amount of the small fibril fraction after centrifugation during nanofibril sample preparation for spin-coating. The supernatant concentration was 1.2 g/L for the HC fibrils compared to 0.4 g/L for the LC fibrils. The thickness of the LC and the HC films was determined to be 6 nm and 4 nm, respectively, by scratching the film with a needle, scanning the scratch using AFM and analysing the height profile. However, further ellipsometry experiments showed a thickness of 11 nm for both LC and HC films (see chapter 4.6.1). The lower thickness values obtained with the AFM scratching method can be due to compression of the samples during the measurements. In addition, the AFM film scratching technique breaks the film and the substrate which can cause a small error in the obtained results.

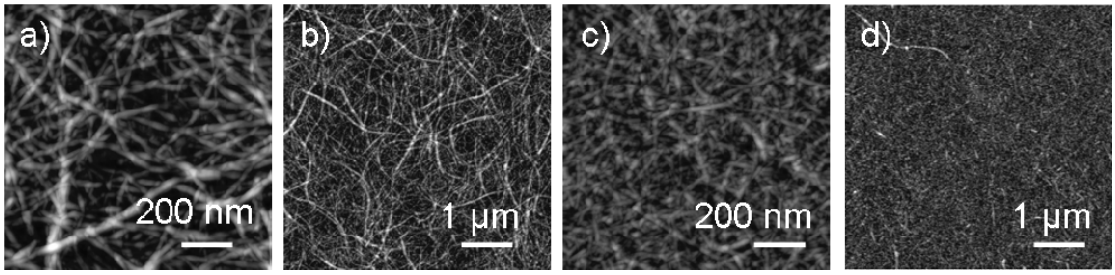

Figure 11. *AFM height images of cellulose nanofibril model films spin-coated on silica substrates (Paper II). (a), (b) Low charged nanofibril surface. APTS was used as an anchoring substance. (c), (d) Highly charged nanofibril surface. The scan size is 1µm×1µm (a, c) and 5µm×5µm (b, d).*

XPS was used to characterise the chemical composition and coverage of the films. The relative atomic concentrations of oxygen, carbon, nitrogen, silicon and carboxylic groups for the model films and their reference substrates are shown in Table 1. The decrease in silicon describes the coverage of the fibrils. For both films, the amount of silicon (and also nitrogen for the LC film) decreases, indicating that the fibrils are covering the substrate. The reduction in Si is larger in the case of the HC film which correlates with the AFM observations which showed that the structure of the HC film is denser than the structure of the more open LC film. The amount of carboxylic groups is higher for the HC film because of the high amount of carboxylic groups in the fibrils. However, the surface composition from elastic peaks showed that there was still some silicon detected from the substrates. Peak-to-background ratios (D) for the Si 2p were therefore calculated. A clear decrease in D ratio is observed for both films, which indicates that the surface is covered with a film thinner than the XPS analysis depth. This correlates with the AFM results and it can be concluded that the observed Si can be explained by the inelastic scattering through the thin films.

Table 1. *Relative atomic concentrations of oxygen, carbon, silicon, nitrogen and carboxylic groups for low-charge and high-charge cellulose nanofibril model films and their references.*

Material	<O>	<C>	<Si>	<N>	<COO>	D
APTS	23.9	45.9	21.8	8.4	0.28	12.3
LC cellulose film	28.7	52.8	13.2	5.3	0.05	10.7
SiO_2	37.4	6.3	56.3	-	0.36	16.9
HC cellulose film	40.4	42.0	17.7	-	0.97	11.4

4.3 Interactions of nanofibril model films with water

Cellulose products are in contact with aqueous solutions or humid conditions in many applications, so understanding the swelling and interactions of cellulose nanofibrils in aqueous environment is of great interest. In Paper II, the interactions of the nanofibril films with water were studied using QCM-D and AFM force measurements. Furthermore, the effect of charge density, electrolyte concentration, and pH on swelling and surface interactions was studied.

Preliminary QCM-D experiments showed that the nanofibril films were stable in water i.e. the films were not detached from the substrates upon exposure in water (Paper II). Heat-treatment of the films was shown to strongly affect the stability of the films. If the films were not heat-treated after spin-coating, the films detached from the substrate upon exposure in water, whereas heat-treated films remained on the substrate. However, a slight increase in frequency was observed for heat-treated LC and HC films as water was injected into the QCM-D chambers indicating that some loosely bound fibrils desorbed from the surface. AFM measurements of the nanofibril films after the QCM-D measurements revealed a fully covering nanofibril surface, further indicating that the nanofibril films are irreversibly attached on the surface. In other words, expect some loosely bound fibrils, the films are not desorbed during the measurements and can be used for the QCM-D measurements.

4.3.1 Effect of electrolyte concentration on swelling and surface interactions

The effect of the electrolyte concentration on nanofibril swelling was studied at pH 8 using QCM-D, see Figure 12. The films were stabilised in water until a stable baseline was achieved, after which, at (t) = 38 min, 1 mM $NaHCO_3$ buffer solution was injected. The buffer addition caused water uptake in both films, but the water uptake was more pronounced for the HC film. This was seen as a decrease in frequency and an increase in energy dissipation as water penetrated inside the film and the film became more viscous. Addition of 1 mM NaCl did not significantly change the swelling of the films, whereas an addition of 10 mM NaCl caused deswelling of the films, i.e. an increase in frequency and a decrease in dissipation were observed. Again, the effect was more pronounced for the HC film. Addition of 100 mM NaCl solution caused further deswelling of the HC film. These changes in frequency can partly be due to the changes in the bulk solution properties i.e. the change in density and viscosity of the electrolyte solution as the concentration is increased. The changes in frequency (for silica) due to the bulk effect were measured to be 1.8 Hz and 9 Hz for 10 mM and 100 mM NaCl solution, respectively. Hence, the small changes observed for the LC films can partly be due to the bulk effects but the bulk effect can not explain the large changes which were observed for the HC films. Similar observations concerning the swelling of regenerated cellulose films were made by Fält et al. (2003), who also showed that the swelling of the regenerated cellulose model surfaces was similar to the swelling of pulp fibres. The increase in electrolyte concentration causes an increase in pH inside the film, which is known as the Donnan effect (Donnan 1911, Grignon and Scallan 1980). Because of the increased pH in the film more carboxyl groups are dissociated, which causes an increase in swelling forces. The more charges there are in the cellulose film, the more the film will swell. However, at higher electrolyte concentrations the osmotic pressure decreases and leads to deswelling of the films.

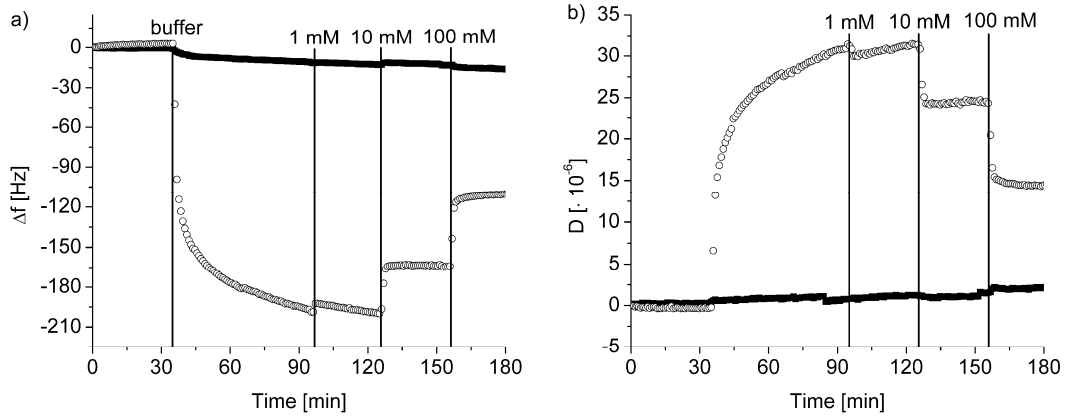

Figure 12. *QCM-D data (3rd overtone) showing the effect of electrolyte concentration on swelling of nanofibril model films (Paper II). Change in (a) frequency and (b) dissipation for low charged (black squares) and highly charged (open spheres) nanofibril films at pH 8.*

The effect of the electrolyte concentration on surface forces between the nanofibril films and a cellulose sphere were studied by AFM to gain an understanding of the nature of interactions when nanofibrillar cellulose is used as a model surface (Paper II). The force measurements indicated that the force profile is due to a combination of steric and electrostatic forces. The observed electrosteric forces were due to the water-swollen and gel-like nature of the nanofibril films which have protruding chains towards the aqueous solution. These results correlate with the QCM-D swelling measurements, which showed that upon swelling the films form highly viscous and highly water-containing structures.

4.3.2 Effect of pH on swelling and surface interactions

The swelling of the nanofibril surfaces in the pH range 3.5-10 was studied using QCM-D. The films were stabilised in 1 mM NaCl solution at pH 5 until a stable baseline was achieved, after which solutions with pH values of 3.5, 5, 8, or 10 were injected. The swelling of the LC nanofibril film did not change at low pH (3.5 and 5), as shown in Figure 13a. At pH 8 the LC film started to swell, which was observed as a decrease in frequency (Figure 13a) and an increase in energy dissipation (Figure 13c). The most extensive swelling was achieved at pH 10. The swelling of the HC film

(Figures 13b and 13d) was similar to the swelling of the LC film, but more pronounced. In addition, at pH 3.5 deswelling occurred, which was observed as an increase in frequency and a decrease in dissipation. In general, the swelling of the HC film was very intense, indicating that the swollen film is very loose and viscous. This is due to the higher amount of carboxyl groups in the HC fibrils. At higher pH values (8 and 10) the degree of dissociation is higher for the carboxyl groups, which causes swelling of the films. This behaviour differs from the swelling of cellulosic fibres which have an apparent pKa value already in the lower pH region (Laine et al. 1994). The dissociation of charged groups in the nanofibril films at higher pH values (pHs 8 and 10) is suggested to be due to closed packing of the charges within the film, which affects the swelling capacity of the films at higher pH.

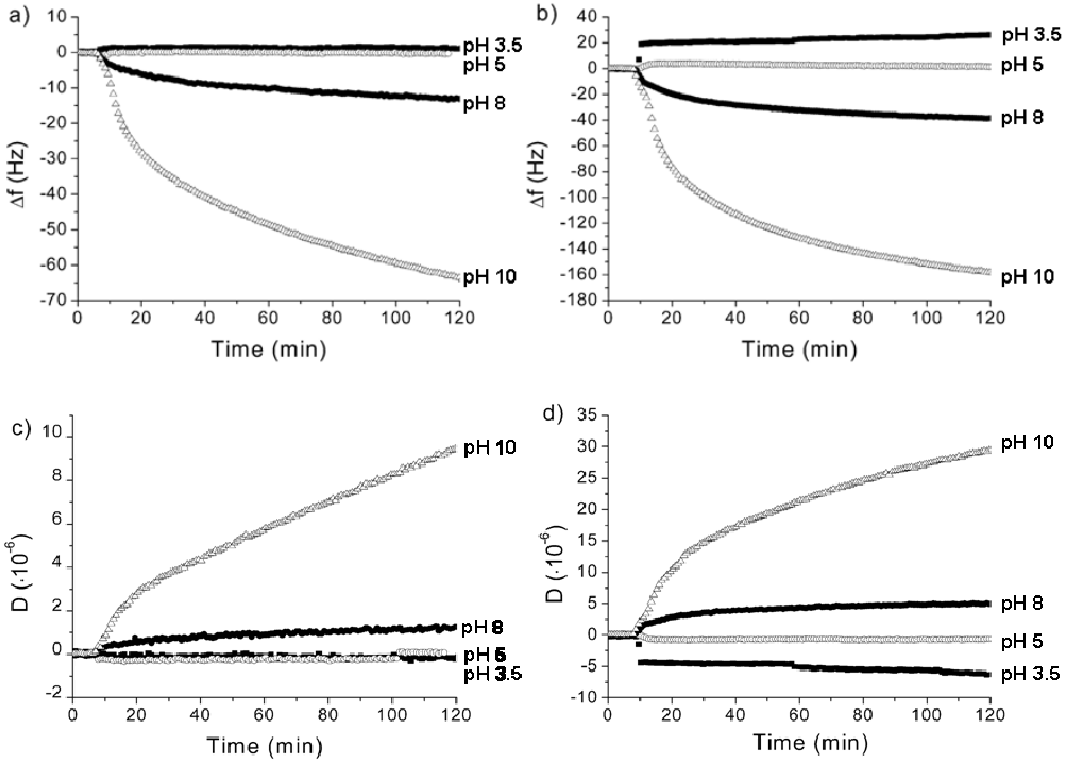

Figure 13. *QCM-D data (3rd overtone) showing the effect of pH on swelling of nanofibril model films. Change in (a, b) frequency and (c, d) dissipation for low-charge (a, c) and high-charge (b, d) nanofibril films in 1 mM NaCl solution. pH values of the solutions were 3.5 (black squares), 5 (open spheres), 8 (open triangles), and 10 (black spheres).*

Surface interactions between cellulose spheres and the nanofibril surfaces were also studied as a function of pH. As pH increased, the repulsion between cellulose surfaces increased, as shown for the HC film in Figure 14. The repulsion is due to dissociation of more carboxylic groups as the pH increases, which was also observed in the QCM-D measurements. This led to an increase in the surface potential of the film but also to an increase in steric repulsion due to the more swollen nanofibril film. Because of the steric repulsion the forces fitted poorly to the DLVO theory. A similar trend was observed for the LC film, though the forces varied notably in magnitude, especially from region to region. It is noteworthy that swelling of the cellulose sphere also affects the observed phenomena but this effect should not significantly change the relative differences between the observed results at different pHs. The effect of pH on the interaction between cellulose surfaces has been previously reported (Carambassis and Rutland 1999, Österberg and Claesson 2000, Poptoshev et al. 2000, Notley et al. 2004, Notley and Wågberg 2005, Notley et al. 2006, Eriksson 2006) and an increase in steric repulsion at higher pHs has been found. The force measurements also correlate with the QCM-D measurements which showed that swelling of the films occurred at pHs 8 and 10, whereas the dissipation values indicated a very viscous and loose structure of the swollen films. This structural change upon swelling explains the observed increased steric repulsion at the higher pH regime.

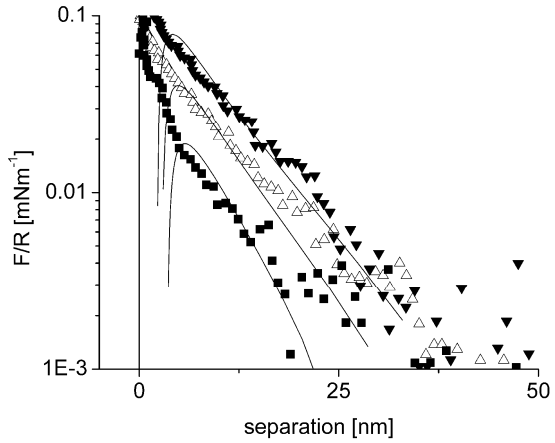

Figure 14. *AFM force curve showing the effect of pH on interactions between approaching cellulose sphere and highly charged cellulose nanofibril surface. pHs studied were 3.5 (■), 8 (△) and 10 (▼) and the lines represent the DLVO theory assuming constant charge (Paper II).*

Based on the swelling and surface interaction studies it can be concluded that generally the swelling behaviour of the cellulose nanofibril model films is similar to the swelling behaviour of cellulosic fibres and regenerated cellulose model surfaces. However, the fibrillar gel-like structure with possible entangling fibrils towards the aqueous solution affects the magnitude of swelling and the importance of steric forces in the interactions.

4.4 Interaction of cellulose nanofibrils with polymers

Several possible applications of cellulose nanofibrils include mixing cellulose with other materials, especially polymers. Strategies to mix nanofibrils and polymers include layer-by-layer deposition (Wågberg et al. 2008, Aulin et al. 2008, Paper IV) or complex formation (Paper IV). The nature of the interaction between cellulose and polymers is strongly affected by the polymer properties, i.e. functional groups, charge properties, molecular weight, structure, etc. (Wågberg 2000). Furthermore, the type of interaction affects the properties of the nanofibril/polymer layer or complex. In the experiments reported in Paper III three different types of polymer were adsorbed on nanofibril model surfaces and the layer properties of the adsorbed films were studied using QCM-D and SPR. A cationic polyelectrolyte, poly (diallyldimethylammonium chloride), PDADMAC, a neutral polysaccharide (xyloglucan), and an anionic cellulose derivative (CMC) were used in the study. The polymers were chosen because it was known from previous studies that they have different effects on cellulose fibre flocculation. PDADMAC is a synthetic flocculating polyelectrolyte which adsorbs on cellulose through strong electrostatic interaction and forms dense adsorbed layers (van de Ven 2000). Xyloglucan and CMC adsorb onto cellulose through glucose-glucose attraction which occurs via hydrogen bonding (Zhou et al. 2007). However, CMC has an electrostatic repulsion to cellulose and irreversible adsorption on cellulose requires higher temperature and high electrolyte concentration (Laine et al. 2000). Both xyloglucan and CMC have been shown to have a dispersing effect on cellulose (Yan et al. 2006, Zhou et al. 2007, Beghello 1998).

Figure 15 shows QCM-D curves where PDADMAC, xyloglucan and CMC are adsorbed on cellulose nanofibril model surfaces. The surfaces were stabilised in an electrolyte solution (1 mM NaCl in 1 mM $NaHCO_3$, pH 8) until a horizontal baseline was obtained. During this stabilization step the films swelled extensively, as was shown in experiments described in Paper II. The decrease in frequency upon swelling is about 80 Hz. At (t) = 10 min the polymer solution is injected. The polymer injection causes different kinds of responses to the frequency and dissipation profiles depending on the polymer used. The adsorption of xyloglucan produces a decrease in frequency and an increase in dissipation, indicating that the polymer and probably

also more water bind to the surface. The adsorption is rather slow and it does not reach equilibrium within the time range studied. Similar adsorption profiles for xyloglucan on regenerated cellulose surfaces have been obtained by Bodin et al. (2007b). CMC addition causes a slow decrease in frequency and an increase in dissipation, indicating that the polymer and water slowly interact with the surface. However, buffer rinsing of the surface after the polymer adsorption causes desorption of CMC, i.e. the frequency increases to the zero level, indicating that all the CMC desorbs from the surface. The injection of PDADMAC causes a sudden increase in frequency and a decrease in dissipation, indicating mass reduction and stiffening of the surface. Since it has been shown that PDADMAC has an electrostatic attraction to cellulose (Wågberg 2000), the mass decrease of the sensor surface is suggested to be due to removal of water from the swollen nanofibril film as the PDADMAC adsorbs on the surface (Saarinen et al. 2009).

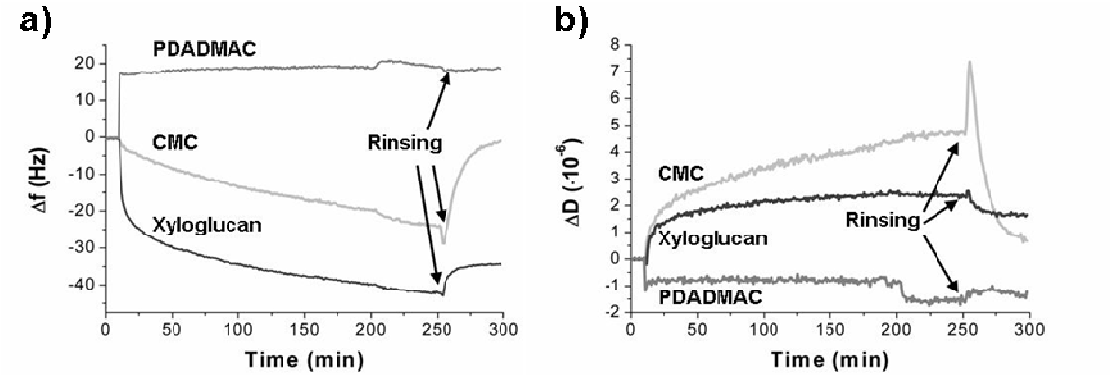

Figure 15. *QCM-D data (3rd overtone) showing the change in frequency a) and dissipation b) upon adsorption of xyloglucan, CMC, and PDADMAC on cellulose nanofibril model surfaces (Paper III). The polymer concentration is 100 mg/L (1 mM NaCl in 1 mM $NaHCO_3$, pH 8).*

As shown in the QCM-D experiments reported in Paper II, water uptake was observed for the nanofibril film at pH 8, indicating a swollen and high-water-content film structure. The presence of water in the nanofibril film is characteristic of the nanofibril material and thus the effect of polymer adsorption on the water content of the film is of great interest. The QCM-D results showed that the type of interaction between substrate and polymer affects the nanofibril-polymer layer properties.

Xyloglucan adsorbs onto the cellulose surface through glucose-glucose attraction. Upon adsorption the energy dissipation increases, indicating softening of the film as more water is bound into the film. Similar effect was observed for CMC although the adsorption was not irreversible in the conditions used. The QCM-D results indicate that xyloglucan and CMC have a dispersing effect on cellulose nanofibrils. These results correlate with previous studies made for cellulosic fibres where xyloglucan and CMC were shown to have dispersing effects on cellulose (Yan et al. 2006).

PDADMAC has an opposite effect on the nanofibril film properties. The strong electrostatic interaction between PDADMAC and nanofibrils densifies the film and results in water removal from the layer. This can be partly caused by charge neutralisation on the fibril surface as highly cationic PDADMAC adsorbs on anionic cellulose nanofibrils. The charge neutralisation leads to a reduction in the swelling forces and results in flattening of the entangled nanofibril network. In addition, in the swollen state the hydroxyl groups in cellulose nanofibrils bind water through hydrogen bonding. Upon xyloglucan and CMC adsorption the amount of hydrogen bonds between the cellulose surface and water is not decreased. PDADMAC does not bind water like xyloglucan and CMC. Upon PDADMAC adsorption the nanofibrils have fewer opportunities to form hydrogen bonds with water and hence, deswelling is observed. Similar effects have not been observed for less-swollen low charged regenerated cellulose films; the PDADMAC adsorption on low charged cellulose causes a decrease in frequency and increase in dissipation upon adsorption (Notley 2008, Tammelin et al. 2006, Saarinen et al. 2009). For highly anionic carboxymethylated regenerated cellulose films Notley (2008) also observed water removal upon PDADMAC adsorption. The results indicate that the low charged cellulose nanofibrils act similarly to highly charged cellulose due to the entangled and highly swollen network structure of the nanofibrils.

Since QCM-D does not give the dry adsorbed mass of the polymers, the interpretation of the adsorbed amount is challenging because of the large amount of water present in the adsorbed layers. Especially the adsorbed amount of PDADMAC was impossible to determine using QCM-D. Thus, SPR was used to determine the dry adsorbed mass of xyloglucan and PDADMAC on nanofibril surfaces. Because of desorption of CMC in the QCM-D experiments and risk of contamination due to high molecular weight of

the CMC studied, it was not used in the SPR adsorption experiments. The same conditions as in the QCM-D measurements were used, i.e. 100 mg/L polymer solution in 1 mM NaCl and 1mM $NaHCO_3$ at pH 8. The nanofibril surfaces were stabilised in the buffer solution before injecting the polymer solution. Injection of both xyloglucan and PDADMAC caused adsorption of the polymers, as shown in Figure 16. The dry adsorbed masses of xyloglucan and PDADMAC from the SPR measurements were about 0.4 mg/m^2 and 0.2 mg/m^2; i.e. the adsorbed mass was twofold higher for xyloglucan. The total adsorbed mass of water and polymer from the QCM-D results was calculated by the Sauerbrey equation (1). The changes in frequency for xyloglucan and PDADMAC correspond to mass changes of 2.5 mg/m^2 and -1.1 mg/m^2, respectively. It is noteworthy that the adsorbed mass values are not equilibrium values. The values are used to compare the adsorbed amounts of the xyloglucan and PDADMAC at (t) = 30 min. The QCM-D and SPR results indicate that the water content of the adsorbed xyloglucan layer is about 80%. Because of the negative total adsorbed amount of PDADMAC in the QCM-D experiments, the corresponding percentage could not be determined. However, because PDADMAC adsorbs with a flat conformation and the adsorbed layer is much denser than the xyloglucan layer, the PDADMAC layer is believed to have significantly lower water content. Thus, combined QCM-D and SPR results shed further light on the effect of the polymer type on layer properties and the water binding capacity of the nanofibril/polymer mixture.

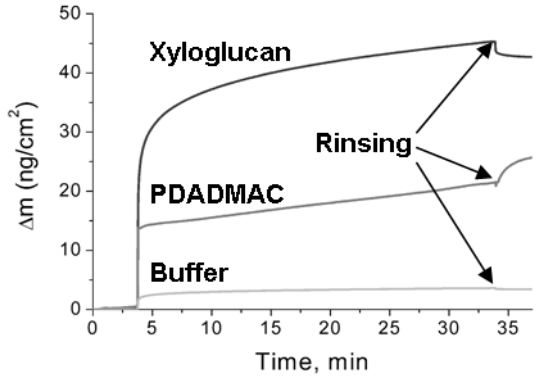

Figure 16 *SPR data showing adsorption of xyloglucan and PDADMAC on cellulose nanofibril model surfaces (Paper III). The polymer concentration is 100 mg/L (1 mM NaCl in 1 mM $NaHCO_3$, pH 8).*

To further study the nanofibril/polymer interactions, aggregated nanofibril suspensions were treated with xyloglucan, PDADMAC and CMC, and the aggregate structure of these nanofibril/polymer mixtures was characterised using confocal microscopy, see Figure 17. The images showed that the reference nanofibril suspension is strongly aggregated and no individual smaller aggregates or fibril bundles can be seen. Compared to the reference, the xyloglucan/nanofibril mixture shows significantly smaller aggregate size throughout the sample. Xyloglucan has a dispersing effect on nanofibrils as was already suggested by the QCM-D results and which further correlates with the observations of Yan et al. (2006). PDADMAC and CMC did not have such a strong effect on the nanofibril aggregation. PDADMAC addition introduced a fraction of smaller aggregates and fibril bundles into the suspension but also larger dense fibril aggregates were present. The dispersing effect was unexpected because PDADMAC is used as a fixative in paper industry (McNeal et al. 2005). This partial dispersing effect can be due to electrostatic repulsion between the fibrils when PDADMAC adsorbs on the surfaces and renders the aggregate cationic (Poptoshev and Claesson 2002). In addition, PDADMAC polymer chain is linear, relatively short and highly charged and thus, in the conditions used here, PDADMAC is not able to further flocculate the already aggregated nanofibril suspension. CMC addition introduced a small dispersing effect but not as strong as that observed with xyloglucan. This is because CMC did not irreversibly adsorb on nanofibrils and in dilute suspensions it is difficult to observe the dispersing effects of CMC. However, it has been shown in earlier studies that CMC can be irreversibly attached on cellulose at higher temperatures and higher salt concentrations (Laine et al. 2000). In that case, the sorption of CMC on cellulose nanofibrils leads to a stronger dispersing effect similar to the effect of xyloglucan (Yan et al. 2006).

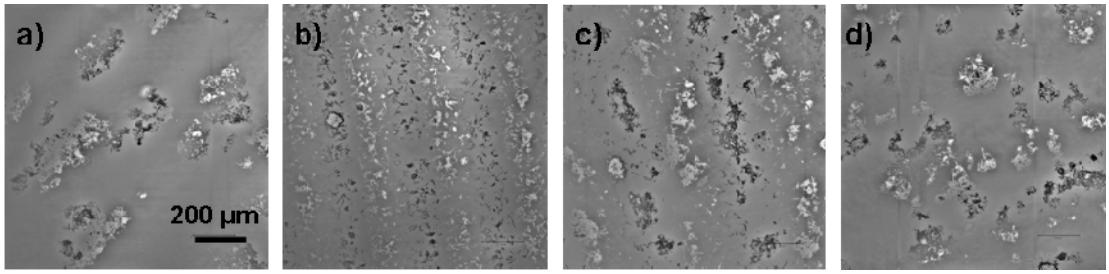

Figure 17 *Confocal microscopy images of a) aggregated cellulose nanofibrils, fibrils mixed with b) xyloglucan, c) PDADMAC, and d) CMC (Paper III).*

The type of the polymer used was shown to have a strong effect on nanofibril film layer properties on the interfacial level, but it also affected the nanofibril suspension aggregation on a more macroscopic level. If nanofibrils are mixed with polymers in novel applications in materials science, it is essential to optimise the water binding capacity of the mixture by choosing the right type of polymer interaction. Furthermore, it is important in nanotechnology applications to have stable, well-dispersed mixtures in order to stay at the nanoscale and avoid unwanted flocculation of the substances. This can be achieved by using dispersing polymers or also by optimizing the nanofibril/polymer charge ratio in order to have electrostatic stabilization of the suspension.

4.5 Application of cellulose nanofibrils as a paper strength additive

To show the potential of cellulose nanofibrils as a reinforcement agent, cellulose nanofibrils were used together with a cationic polyelectrolyte, poly(amideamine) epichlorohydrin (PAE), to enhance paper strength (Paper IV). PAE is widely used in the paper industry as a wet strength agent. It reacts with cellulose during or after paper drying through a hetero-crosslinking reaction between 3-hydroxy-azetidinium groups of PAE and the carboxyl groups of cellulose (Espy 1995, Wågberg and Björklund 1993). Highly anionic cellulose nanofibrils were used in the study to maximise the reactive sites between cellulose and PAE. The differences in fibril and polymer adding strategies were studied by comparing layer-structures and nano-aggregates formed by the nanofibrils and PAE.

To understand the interactions on a fundamental level, the adsorption of HC nanofibrils and PAE on LS cellulose model surfaces was studied using QCM-D and AFM imaging. Figure 18 shows QCM-D adsorption curves where PAE and nanofibrils are adsorbed on cellulose as a layer structure (Figure 18a) or as pre-formed nano-aggregates (Figure 18b). Preliminary experiments showed that nanofibrils do not adsorb on cellulose model surfaces as such. However, when cationic PAE is first adsorbed on the cellulose model surface, nanofibrils can then be adsorbed on the PAE layer (Figure 18a). PAE adsorption causes a rather small increase in energy dissipation, indicating a flat and rigid adsorbed layer, while nanofibril adsorption

causes a considerable increase in dissipation, indicating a very loose and viscous adsorbed layer. When PAE and nanofibrils are injected as cationic nano-aggregates (PAE:nanofibril charge ratio 3:1), a decrease in frequency and an increase in energy dissipation are observed as the aggregates adsorb on cellulose (Figure 18b). The total adsorbed amount of aggregates is rather small compared to the adsorbed amount of the PAE-nanofibril bilayer system. The increase in energy dissipation is also much lower, indicating a dense layer. The higher adsorbed amount in sequential adsorption is assumed to be partly due to the higher amount of coupled water in the layer, which can also be observed as high dissipation values. A possible explanation for the extremely high dissipation values is that the nanofibrils adsorb as a network-structured interface where the high-aspect-ratio fibrils are anchored to the PAE layer through electrostatic attraction, but the repulsion between the fibrils inside the layer inhibits close packing of the material and this orientation causes the high dissipation values.

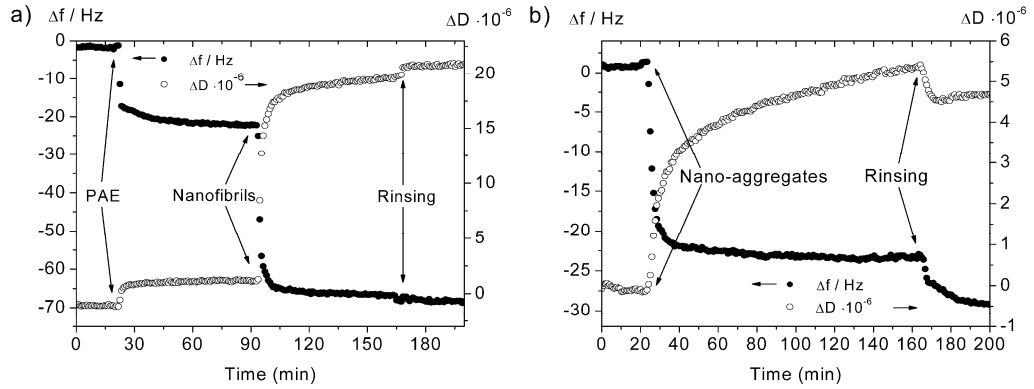

Figure 18. *QCM-D data (3rd overtone) showing the change in frequency and dissipation upon adsorption of PAE and nanofibrils as a) a sequential adsorption and b) pre-mixed PAE-nanofibril aggregates on LS cellulose model surfaces (Paper IV). PAE, nanofibrils, and aggregates were adsorbed from 100 mg/L solutions in 0.1 mM NaCl and 1 mM $NaHCO_3$.*

The QCM-D crystals used in the adsorption studies were imaged with AFM to verify the adsorption of PAE and nanofibrils on the LS cellulose model surfaces. Figure 19 shows AFM height images of a pure LS cellulose surface (a), the surface after the sequential adsorption of PAE and nanofibrils (b), and the surface after the adsorption

of the PAE-nanofibril aggregates (c). It can be seen from Figure 19b that the sequential adsorption results in a homogeneously distributed open film of nanofibrils on the substrate, whereas the adsorbed PAE-nanofibril aggregate layer in Figure 19c shows a heterogeneous adsorbed layer where large aggregates and empty spots are visible. Thus, it can be concluded that the sequential adsorption leads to more controlled and homogeneous distribution of the substances than the nano-aggregate adsorption strategy.

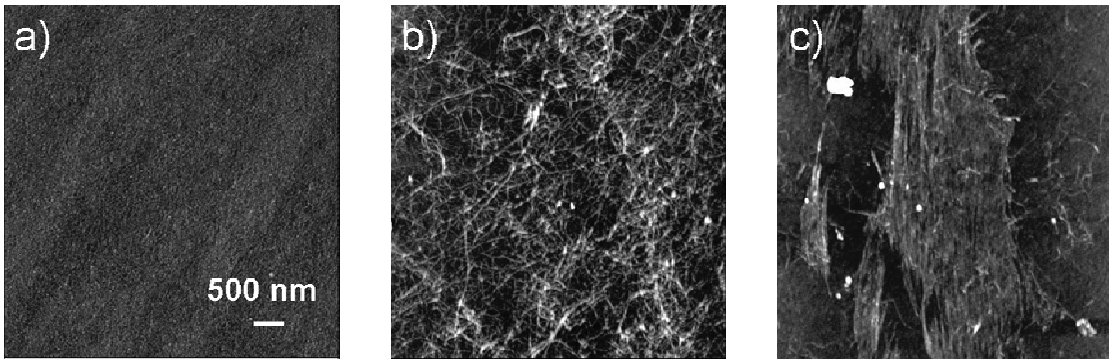

Figure 19. *AFM height images of a) plain LS cellulose model film, b) LS cellulose film after sequential adsorption of PAE and cellulose nanofibrils, c) LS cellulose film after the adsorption of PAE-nanofibril 3:1 aggregates. The scan size of the images is 5 ×5 µm and the Z-range is 20 nm (Paper IV).*

Paper sheets were prepared from delignified softwood pulp fibres which had been treated with PAE and nanofibrils using either the sequential adsorption of PAE and the nanofibrils on the pulp fibres, or the nano-aggregate adsorption strategy, where pre-mixed PAE-nanofibril aggregates were mixed with the pulp slurry. Figure 20 shows the wet and dry tensile strength index of paper sheets as a function of the added amount of the nanofibrils at a constant amount of PAE. In sequential adsorption both the wet and dry tensile strength increase significantly as the added amount of nanofibrils increases. The adsorption of nano-aggregates also causes an increase in strength properties, but the strength values are lower than what was observed in sequential adsorption. This can be partly due to the fact that when nanofibril addition exceeds 20 mg/g the aggregates are anionic. Because of the lack of electrostatic attraction between the aggregates and the fibres and because of repulsion between the aggregates, they do not adsorb onto the fibres. Another reason behind the lower

strength values can be uneven distribution of the aggregates on fibre surfaces, as was also suggested by the AFM measurements.

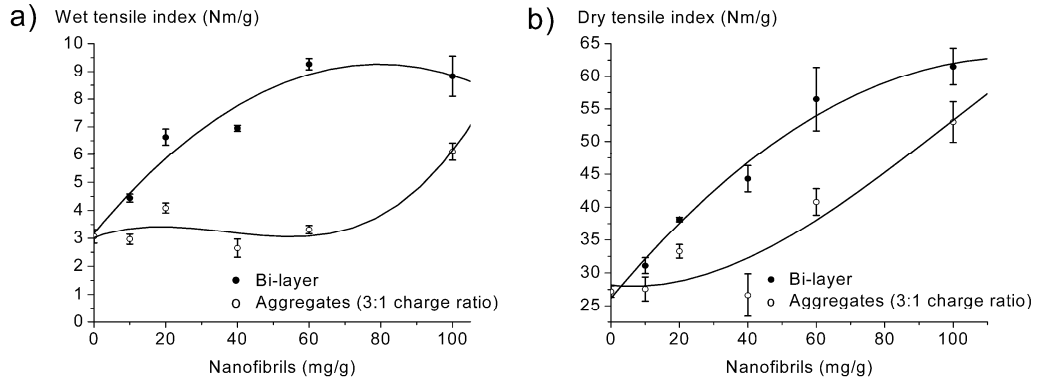

Figure 20. *a) Wet tensile index and b) dry tensile index of paper made from delignified softwood pulp treated with PAE (5mg/g) and cellulose nanofibrils at pH 8 (Paper IV).*

The paper strength development was also studied as a function of PAE addition when nanofibril addition was kept constant (60 mg/g). The adsorbed amount of PAE was determined by bulk nitrogen analysis which correlates with the amount of PAE in the paper sheets. Figure 21 presents the wet tensile strength as a function of the bulk nitrogen content of the paper sheets. For the reference samples where only PAE is added the wet strength is almost constant, even though the bulk nitrogen content increases. The reason for this may be that already at small PAE additions all the sites to form covalent bonds with the pulp fibres are utilised. When more PAE is added the polymers attach only electrostatically on the surface and due to lack of covalent bonding the wet strength properties are not further improved. In sequential adsorption the wet strength of paper sheets significantly increases up to 0.4 mg/g nitrogen content, after which it starts to decrease. The decrease may be due to aggregation of PAE and nanofibrils before they are adsorbed on the pulp fibres, which affects the distribution of the substances on the fibre surfaces. When PAE and nanofibrils are added as aggregates no linear effect on wet strength is seen and the values are close to the values of the reference PAE samples. A maximum value is achieved at 0.3 mg/g nitrogen content. This may also be due to further aggregation of the particles at higher dosages. It is evident from the results that the strategy how the nanofibrils are added

strongly affects the strength development of paper. At similar adsorbed amounts of PAE, i.e. similar nitrogen contents, the sequential adsorption gives significantly higher strength values than the nano-aggregate adsorption. This is due to more uniform distribution of the substances when PAE and nanofibrils are adsorbed as a bilayer system. Nanofibrils not only offer more adsorption sites to PAE but the carboxyl groups in the nanofibrils also offer reaction sites to PAE to form covalent bonds which are needed for the wet strength development. In addition, PAE is more concentrated to the surface in the sequential adsorption system. The nanofibrils themselves may also have a strength enhancement effect and the highly water-containing network-structure of the nanofibrils increases surface area on the fibre surfaces resulting in improved bonding properties of the fibres. Hence, it can be concluded that the addition strategy does not affect the total adsorbed amount of PAE but it strongly affects the distribution of the substances, which has a crucial effect on paper strength development.

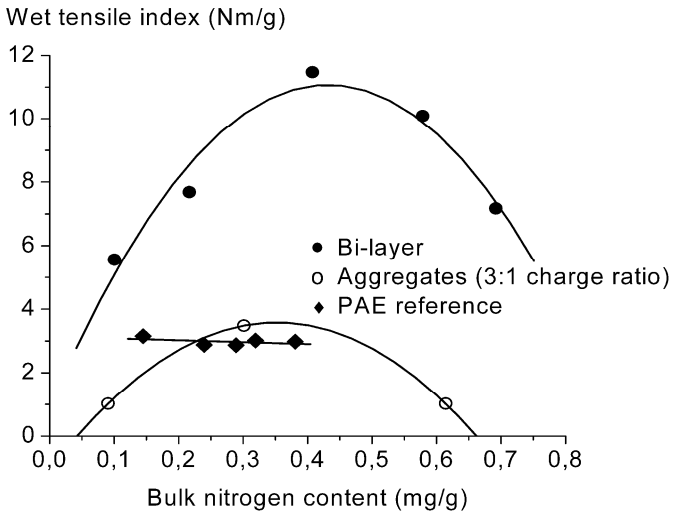

Figure 21. *Wet tensile index of paper as a function of bulk nitrogen content (Paper IV). The hand sheets were made from delignified softwood fibres treated with PAE (1-10 mg/g) and cellulose nanofibrils (60 mg/g).*

The results in Paper IV showed that nanofibrils can be used together with PAE to improve paper strength. It is noteworthy that addition of nanofibrils may affect dewatering in papermaking, because the adsorbed layers contain much water. However, during hand sheet preparation slight changes in dewatering times were

observed only with the highest amounts (100 mg/g) of nanofibrils. At the optimum dosage (60 mg/g) no such changes were observed. In addition, industrial-scale production of nanofibrils remains to be developed. On the other hand, using nanofibrils together with PAE is a superior combination to improve both wet and dry strength of paper compared to other suggested systems for using PAE together with an anionic polyelectrolyte to improve paper strength (Laine et al. 2002, Gärdlund et al. 2003). However, the surface chemical phenomena related to adsorption and aggregate formation need to be well understood in order to achieve optimal improvements in paper quality and process efficiency.

4.6 Comparison of cellulose nanofibril films with other cellulose model films

The cellulose nanofibril film, which was developed and described in Paper II, acts as a model for cellulose nanofibril materials. Due to the native origin of the cellulose nanofibrils, the film can also be used as a model for the surface of native cellulose fibres, which contain both amorphous and crystalline regions. In this chapter the properties of cellulose nanofibril film were compared with properties of other cellulose model films. Special attention was paid to the effect of model film suprastructure and morphology on swelling and enzymatic hydrolysis of cellulose.

4.6.1 Effect of cellulose material crystallinity on interactions with water

One drawback in the earlier cellulose model film research has been the lack of data on the crystallinity and crystal structure of the cellulose constituting these films. This knowledge is required to enable molecular interpretations of the interactions between the films and other specimens. The lack of data has been due to limitations of the methods for determining the crystallinity of thin films. Several attempts have been made to find a representative model surface for cellulose (Paper II, Kontturi et al. 2006). However, the interpretations of cellulose model surface experiments have earlier been based on the assumed crystallinity of the cellulose constituting these surfaces. For example, cellulose nanocrystals have been assumed to be fully or almost fully crystalline, whereas regenerated cellulose films, such as LS cellulose films, have

been assumed to be fully amorphous. To gain a deeper understanding of the cellulose model surfaces, the cellulose model film crystallinity measurements were performed using small incidence x-ray diffraction (unpublished data). The effect of crystallinity on the interaction of cellulose with water was studied using QCM-D. The thickness of the films was determined using ellipsometry. Seven different types of cellulose model film were compared in the study. Regenerated cellulose films studied were spin-coated NMMO and DMAc-LiCl dissolved cellulose and Langmuir-Schaefer cellulose surfaces. Fibrillar cellulose surfaces studied were spin-coated low-charge nanofibril surfaces (NFC), high-charge nanofibril surfaces with PEI as an anchoring polymer (PEI/NFC 1), and high-charge nanofibril and PEI multilayer films with 7 layers (PEI/NFC 7). In addition, spin-coated cellulose nanocrystal films (NC) were studied.

Small angle incidence X-ray diffraction measurements (unpublished data) of the cellulose films showed partly crystalline cellulose I structure for LC and HC nanofibrils, as had been earlier proposed due to the native origin of the fibril materials. Cellulose nanocrystals also showed highly crystalline cellulose I structure, whereas DMAc-LiCl -dissolved regenerated cellulose films showed fully amorphous structure. Surprisingly, the regenerated LS cellulose surface as well as NMMO-dissolved regenerated cellulose surface showed partly crystalline cellulose II structure. The partial crystalline structure of the LS cellulose can be due to re-crystallisation of cellulose through self-assembly in the layered LS film. Re-crystallization of cellulose through self-assembly has also been observed by Yokota et al. (2007). The partial cellulose II crystallinity of NMMO-dissolved cellulose film is due to colloidal nature of the cellulose solution. The cellulose in not fully dissolved in NMMO and the cellulose has a fringe micellar type of arrangement with some aggregates present in the solution (Notley et al. 2006).

The interaction of the cellulose model surfaces with water was studied using QCM-D (unpublished data). The measurements were started in air after which a dilute buffer solution (10^{-5} M $NaHCO_3$) was injected. Figure 22 shows the swelling curves for all the model films studied. The injection of the buffer caused a sudden drop in frequency and an increase in energy dissipation. This was mainly due to the difference in viscosity between air and the aqueous buffer solution but also due to initial water uptake in the cellulose surfaces. After this initial water uptake most of the films did

not swell much more, resulting in a sharp 90° angle shape of the curves. DMAc-LiCl (Fig 22a) and PEI/NFC 7 multilayer film (Fig 22c) swelled the most and the swelling continued for several hours. The change in energy dissipation correlated with the observed changes in frequency. An exception was the LC nanofibril surface (NFC) which showed the highest energy dissipation values (Fig 22c), indicating a very viscous swollen film compared to the quantity of water uptake (Fig 22b).

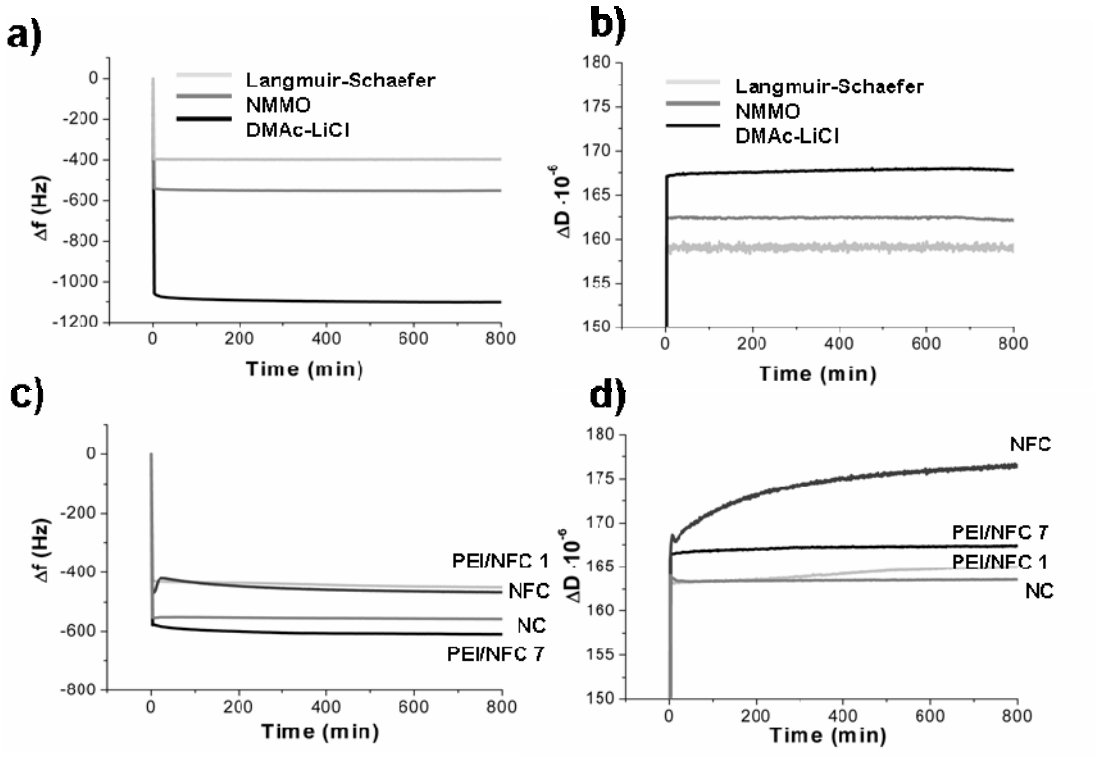

Figure 22. *QCM-D data (3rd overtone) showing the swelling of cellulose model films upon exposure to 10^{-5} M $NaHCO_3$ buffer solution (at t = 0 min). Change in (a, c) frequency and (b, d) dissipation as the films swell in aqueous solution (unpublished data).*

The amount of cellulose in the model surface affects the water uptake in the film, i.e., the more cellulose in the film, the more water can penetrate. Because the cellulose model surfaces studied had varying mass of cellulose and varying thicknesses, the QCM-D raw data results could not be used as such to compare quantitatively the swelling of the surfaces. The swelling percentage (mass of water/dry mass of the film) was determined to exclude the effect of the film thickness and the amount of cellulose in the films, see Table 2. The mass of water was determined using the Sauerbrey

equation and further confirmed with Johansmann's model, because the Sauerbrey equation is known to underestimate the adsorbed mass values for viscoelastic films. The calculations showed that the adsorbed mass was slightly higher when calculated with the Johannsmann's model but the difference was very small. The results indicate that the swelling percentage of the DMAc-LiCl film is very high compared to that of the other films. The LS cellulose and nanofibril/PEI multilayer had the lowest swelling percentages. This was suggested to be due to the density of the films, which prevents the water from penetrating inside the film. The other films studied had fairly similar swelling percentages.

Table 2. *Crystalline form, thickness and dry mass of cellulose model surfaces, adsorbed mass of water, and swelling percentage of the surfaces (unpublished data).*

Surface	**Crystalline form**	**Thickness nm**	**Dry mass of cellulose mg/m^2**	**Adsorbed mass Sauerbrey mg/m^2**	**Adsorbed mass Johanns-mann mg/m^2**	**Swelling %**
NMMO	cellulose II / amorphous	32.5	48.8	11.2	12.1	23
DMAc-LiCl	amorphous	53.8	80.7	40.7	43.0	51
TMSC/LS	cellulose II / amorphous	17.8	26.7	2.1	2.2	8
LC nanofibril	cellulose I / amorphous	11.9	17.9	4.6	5.0	26
HC nanofibril/PEI	cellulose I / amorphous	12.5	18.8	4.2	4.5	23
HC nanofibril/PEI 7 layers	cellulose I / amorphous	75	112.5	12.9	13.8	12
Nanocrystals	cellulose I / amorphous	23.6	35.4	9.9	11.5	28

The supramolecular structure of cellulose affects the swelling of the cellulosic fibres but other features such as the morphology, thickness and density of the model surfaces were shown to affect the swelling phenomena. It has been shown in earlier studies (Müller et al. 2000) that water can penetrate into amorphous cellulose and cause swelling, whereas water cannot penetrate into crystalline cellulose because of

the dense packing of the crystals. The fully amorphous DMAc-LiCl film showed the highest swelling, which correlates with the findings of earlier studies (Notley et al. 2006). However, as shown by the swelling percentages in Table 2, the second highest swelling percentage was obtained for the cellulose nanocrystal surfaces. This indicates that water can penetrate between the nanocrystals and cause swelling of the nanocrystal network. On the other hand, the crystallinity of LS and NMMO films was shown to be quite similar, but the swelling percentage of the LS film was significantly lower than that of the NMMO film. This is due to the dense packing and smooth surface morphology of the LS film (Tammelin et al. 2006), which makes it more difficult for the water to penetrate inside the film. From the swelling results it can be concluded that the swelling of cellulose model films is a complex phenomenon which is affected by a combination of several chemical and physical properties of the films, not only the supramolecular structure of cellulose.

4.6.2 Enzymatic degradation of cellulose films

Enzymatic hydrolysis can be utilised to produce fermentable sugars from cellulose for conversion into biofuels. Fundamental studies on the enzyme-substrate interactions contribute to developing more effective enzyme mixtures. In the work reported in Paper V cellulose nanofibril model surfaces were used to study the enzymatic hydrolysis of cellulose using QCM-D and AFM imaging. A commercial cellulase mixture containing endoglucanases, cellobiohydrolases, and β-glucosidases was used. The enzymatic hydrolysis of nanofibril films was compared to hydrolysis of other cellulose model surfaces with varying supramolecular structure and morphology. Earlier enzymatic hydrolysis studies have been performed on regenerated or fully crystalline cellulose surfaces (Eriksson et al. 2005, Joseffson et al. 2008, Turon et al. 2008). As already noted in chapters 4.2 and 4.6.1, the nanofibril model surface is a representative model of native cellulose because it consists of both crystalline cellulose I and amorphous regions. Hence, this model substrate gave an opportunity to study, at a fundamental level, the enzymatic hydrolysis of native cellulose and it also made it possible to study the effect of model film crystallinity and surface morphology on the hydrolysis dynamics.

QCM-D results showed that the enzymatic hydrolysis of the nanofibril model film is extremely fast for the whole enzyme dosage range (0.01%-0.5%) studied. The hydrolysis was completed in a few minutes, as can be seen from Figure 23a for the 0.5% dosage. Enzyme binding causes a sudden decrease in frequency but the trend is reversed within less than one minute as the enzymatic hydrolysis starts to dominate over the binding as the enzymes start to degrade the available cellulose. The energy dissipation increases when the enzymes start to bind on the surface due to increased viscoelasticity of the films, i.e. the cellulose layers are cleaved and the film becomes more hydrated and swollen. A maximum in the dissipation is reached around the time when the enzymatic hydrolysis starts to slow down for LS and NMMO films whereas for nanofibril and nanocrystal films the dissipation maximum is close to the adsorption maximum. When the enzymatic hydrolysis of the nanofibril surface is compared to LS cellulose film (Figure 23b), NMMO spin-coated film (Figure 23c), and cast cellulose nanocrystal film (Figure 23d), it is evident that the hydrolysis of the nanofibril film is significantly faster than the hydrolysis of the other films. Similar trends for all the cellulose films can be seen but the kinetics differ significantly between the films. The degradation of the LS film is also rather fast compared to the spin-coated NMMO film and especially the cast nanocrystal surface, which shows very slow degradation kinetics, i.e. the degradation takes several hours compared to the few minutes required to degrade the nanofibril film.

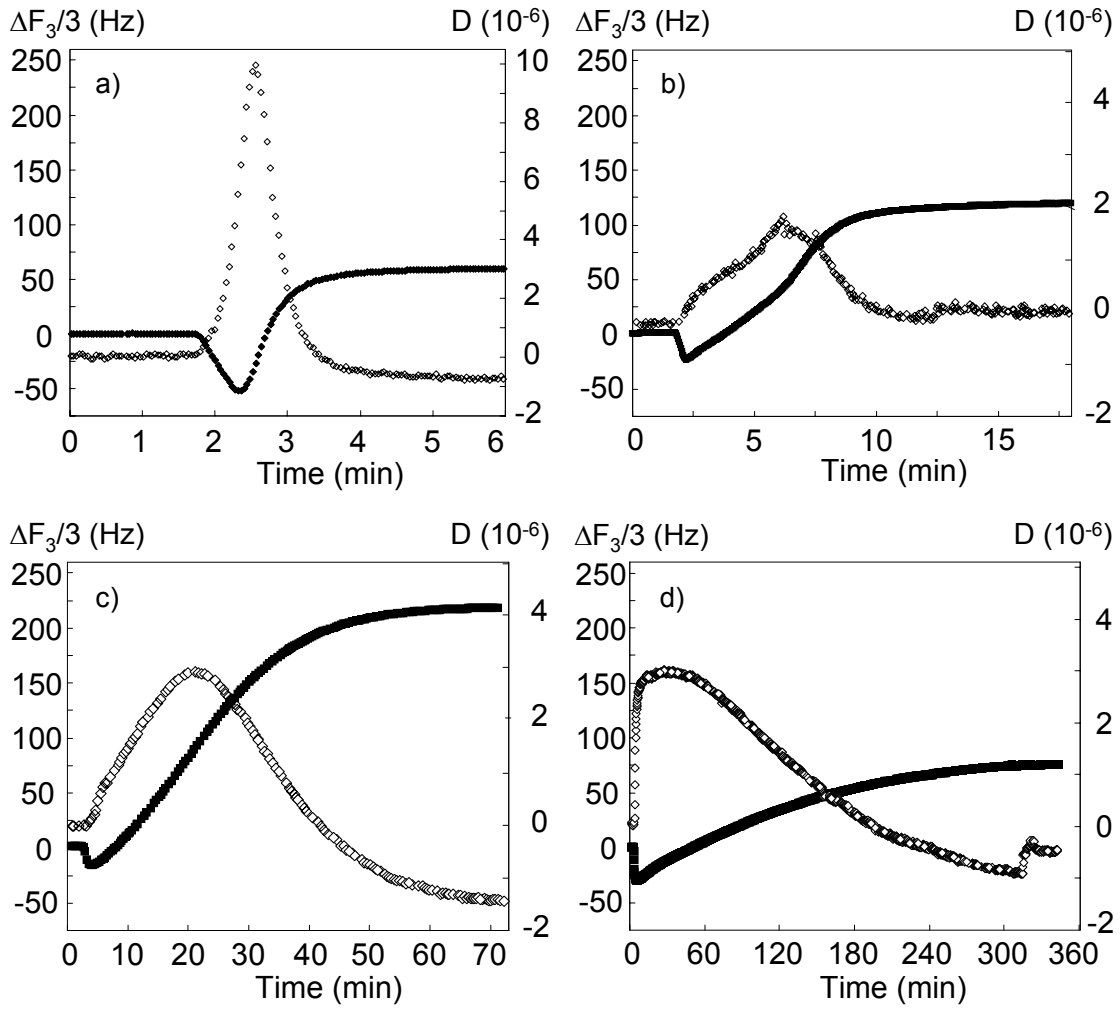

Figure 23. *QCM-D data (3rd overtone) showing the change in frequency (F) and change in dissipation (D), for a) nanofibril, b) Langmuir-Schaefer, c) spin-coated regenerated, and, d) nanocrystal cellulose model film treated with 0.5% cellulase mixture (40 °C and pH 5). Full squares correspond to the frequency plot and empty diamonds to energy dissipation (Paper V).*

The fast hydrolysis kinetics of the nanofibril film is unexpected because the crystalline cellulose I regions are assumed to slow down the degradation when compared to regenerated LS and NMMO cellulose surfaces (Himmel et al. 2007). The fast hydrolysis kinetics is suggested to be due to the large available surface area of cellulose for the enzymes to attack, and also the possible cleavage of whole nanofibril sections. The slow kinetics for the nanocrystal surface is expected because the strong hydrogen bonding network makes the crystalline cellulose resistant to enzymatic hydrolysis. The results were fitted to an empirical model which also showed the

differences in the hydrolysis kinetics, i.e. the rate of hydrolysis was significantly faster for the nanofibril films compared to the LS cellulose, spin-coated NMMO, and especially the cast nanocrystal surface. The empirical model is described more detailed in the reference (Turon et al. 2008) and in Paper V.

AFM imaging of the cellulose surfaces before and after the enzymatic hydrolysis was performed to study the morphological changes that occur during the hydrolysis. Figure 24 shows AFM height images of cellulose nanofibril film, LS cellulose film, spin-coated regenerated cellulose film and cast cellulose nanocrystal film. The cellulose nanofibril film is completely degraded by the enzymes, whereas some remaining LS cellulose can be seen after the hydrolysis. A possible explanation for this can be the occurrence of re-crystallization of amorphous cellulose to cellulose II due to self-assembly during the LS film preparation, as was shown in chapter 4.6.1. The spin-coated NMMO film is completely degraded and a typical substrate structure is observed after the hydrolysis. The nanocrystal surface is not fully degraded and the largest crystal aggregates remain on the surface. This is expected because crystalline cellulose is more difficult to degrade than amorphous cellulose due to strong hydrogen-bonding network, which makes crystalline cellulose resistant to enzymatic hydrolysis. Similar densely packed residues for *endo*-xyloglucanase-degraded xyloglucan films have been observed by Nordgren and co-workers (Nordgren et al. 2008).

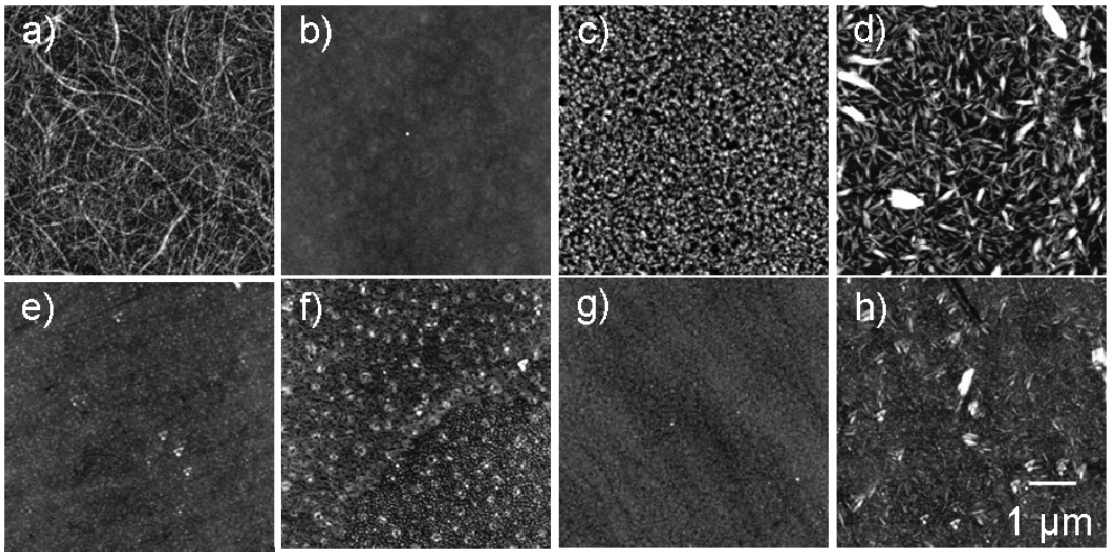

Figure 24. *AFM height images of cellulose nanofibril model films a) before and e) after enzymatic hydrolysis, LS model film b) before and f) after hydrolysis, spin-coated NMMO cellulose film c) before and g) after hydrolysis, and cast nanocrystal surface d) before and h) after hydrolysis. The scan size of the images is 5 ×5 µm and the Z-range is 30 nm, expect for image g) where the Z-range is 50 nm (Paper V).*

Although the supramolecular structure of cellulose was shown to be the most relevant factor affecting the enzymatic hydrolysis of fully crystalline cellulose, it did not determine the hydrolysis kinetics of the nanofibril film. It was shown that the morphology and thickness of the films also affect the hydrolysis of cellulose. The more surface area available for the enzymes to attack, the more effectively the enzymes can reach the inner layers of cellulose. This may have caused the differences in the hydrolysis kinetics between the more open and network-structured nanofibril film and the more densely packed cellulose films. The thickness of the films correlates with the amount of degradable mass of cellulose and hence affects the total time of hydrolysis. The spin-coated NMMO cellulose film is thicker than the LS cellulose film (see Table 2), which may be the reason for the slower hydrolysis kinetics obtained for the NMMO film. Generally, the results showed that while the cellulose films are simple models of real substrates, the chemical and morphological differences play important roles in the overall time evolution of film degradation. QCM frequency and dissipation profiles, in combination with AFM imaging after

substrate incubation, add to our understanding of enzyme adsorption and the mechanism of action.

5 CONCLUDING REMARKS

Cellulose nanofibril materials prepared with novel disintegration methods were characterised in this thesis work. The most characteristic feature of these high-aspect-ratio nanofibrils is the formation of an entangled network which under aqueous conditions forms high-water-content gel-like structures. In this thesis work, the gel-like structure was shown to affect many interfacial phenomena of nanofibrils, such as swelling, surface forces, enzymatic degradability, and adsorption of polymers on nanofibril surfaces.

Novel cellulose model surfaces from cellulose nanofibrils were prepared, enabling further fundamental studies of nanofibril interactions. The films act as a model of nanofibrillar cellulose but also in general as a model of native cellulose containing both crystalline cellulose I and amorphous regions. The swelling of nanofibril films is similar to the swelling of other cellulose model surfaces and cellulosic fibres. However, the high-water-content fibrillar gel-like structure with entangling fibrils towards the aqueous solution affects the magnitude of swelling and the importance of steric forces in the surface interactions.

Polymer adsorption on cellulose nanofibril surfaces is highly dependent on the nature of nanofibril/polymer interaction. The type of adsorbed polymer determines the effect of the adsorbed layer on nanofibril film properties. Adsorption of a neutral polysaccharide caused a dispersing effect of the nanofibrils and water uptake in the film, whereas adsorption of a cationic polyelectrolyte caused water removal and densification of the film. These effects are essential for further applications in nanomaterials science where polymers and nanofibrils are mixed together. The water binding capacity and suspension stability can be optimised by choosing the right type of polymer interaction.

Dynamic rheology measurements showed that the nanofibril gels are very strong, so the material has potential as a strength reinforcing agent in materials science. The potential of cellulose nanofibrils as a strength reinforcing agent was further demonstrated when the nanofibrils were used together with a cationic polyelectrolyte,

PAE, to enhance paper strength. The paper strength experiments together with fundamental interaction studies showed that the use of nanofibrils as a strength reinforcing agent together with PAE leads to superior improvements in strength properties. However, the surface chemical phenomena behind the interactions have to be well understood in order to achieve optimal results. Furthermore, the use of nanofibrils together with PAE in this thesis work is only one example of several possible nanofibril/polymer combinations for strength improvement. Similar systems with different polymers are applicable in paper science and in several applications in nanomaterials science.

Cellulose nanofibril films were compared to different types of cellulose model surfaces to study the effect of cellulose supramolecular structure, chemistry, and surface morphology on enzymatic hydrolysis of cellulose, and on the interactions of cellulose with water. While the cellulose films used are simple models of real substrates, the chemical and morphological differences play an important role in the overall evolution of the enzymatic degradation of cellulose. Crystallinity measurements combined with swelling studies of cellulose model surfaces revealed, surprisingly, that the supramolecular structure of cellulose is not the determining factor in interactions of cellulose model films with water. The physical structure of the model surfaces also has a strong effect and the overall effects are combinations of the chemical and physical factors. These new findings are very important when making molecular interpretations of fundamental cellulose model surface experiments. It is evident that the packing of the cellulose material in the model surfaces is an important factor and more information about cellulose model film densities is needed to fully understand the interfacial phenomena of cellulose model films.

6 REFERENCES

Abe, K., Iwamoto, S., Yano, H. (2007). "Obtaining cellulose nanofibers with a uniform width of 15 nm from wood." *Biomacromolecules,* 9(3), 1022-1026.

Andresen, M., and Stenius, P. (2007). "Water-in-oil emulsions stabilized by hydrophobized microfibrillated cellulose." *J. Dispersion Sci. Technol.,* 28(6), 837-844.

Andresen, M., Stenstad, P., Moretro, T., Langsrud, S., Syverud, K., Johansson, L., Stenius, P. (2007). "Nonleaching antimicrobial films prepared from surface-modified microfibrillated cellulose." *Biomacromolecules,* 8(7), 2149-2155.

Andresen, M., Johansson, L., Tanem, B. S., Stenius, P. (2006). "Properties and characterization of hydrophobized microfibrillated cellulose." *Cellulose,* 13(6), 665-677.

Araki, J., Wada, M., Kuga, S., Okano, T. (2000). "Birefringent glassy phase of a cellulose microcrystal suspension." *Langmuir,* 16(6), 2413-2415.

Araki, J., Wada, M., Kuga, S., Okano, T. (1999). "Influence of surface charge on viscosity behavior of cellulose microcrystal suspension." *Journal of Wood Science,* 45(3), 258-261.

Araki, J., Wada, M., Kuga, S., Okano, T. (1998). "Flow properties of microcrystalline cellulose suspension prepared by acid treatment of native cellulose." *Colloids and Surfaces, A: Physicochemical and Engineering Aspects,* 142(1), 75-82.

Aulin, C., Varga, I., Claesson, P. M., Wågberg, L., Lindström, T. (2008). "Buildup of polyelectrolyte multilayers of polyethyleneimine and microfibrillated cellulose studied by in situ dual-polarization interferometry and quartz crystal microbalance with dissipation." *Langmuir,* 24(6), 2509-2518.

Azizi Samir, M., Alloin, F., Sanchez, J., El Kissi, N., Dufresne, A. (2004). "Preparation of cellulose whiskers reinforced nanocomposites from an organic medium suspension." *Macromolecules,* 37(4), 1386-1393.

Barnes, H. A., Hutton, J. F., Walters, K. (1989). *An Introduction to Rheology,* Elsevier, Amsterdam.

Battista, O. A., Coppick, S., Howsmon, J. A., Morehead, F. F., Sisson, W. A. (1956). "Level-off degree of polymerization. Relation to polyphase structure of cellulose fibers." *Journal of Industrial and Engineering Chemistry,* 48, 333-335.

Beghello, L. (1998). "Some factors that influence fiber flocculation." *Nordic Pulp & Paper Research Journal,* 13(4), 274-279.

Berglund, L. (2005). "Cellulose-based nanocomposites." In *Natural Fibers, Biopolymers, and Biocomposites;* Mohanty, A., Misra, M., Drzal, L., Eds., CRC Press, Boca Raton, FL, pp 807-832.

Berthold, F., Gustafsson, K., Berggren, R., Sjöholm, E., Lindström, M. (2004). "Dissolution of softwood kraft pulps by direct derivatization in lithium chloride/N,N-dimethylacetamide." *J Appl Polym Sci,* 94(2), 424-431.

Binnig, G., Quate, C. F., Gerber, C. (1986). "Atomic force microscope." *Phys. Rev. Lett.,* 56(9), 930-933.

Blodgett, K. B. (1935). "Films built by depositing successive unimolecular layers on a solid surface." *J. Am. Chem. Soc.,* 57, 1007-1022.

Bodin, A., Bäckdahl, H., Fink, H., Gustafsson, L., Risberg, B., Gatenholm, P. (2007a). "Influence of cultivation conditions on mechanical and morphological properties of bacterial cellulose tubes." *Biotechnol. Bioeng.,* 97(2), 425-434.

Bodin, A., Ahrenstedt, L., Fink, H., Brumer, H., Risberg, B., Gatenholm, P. (2007b). "Modification of nanocellulose with a xyloglucan-RGD conjugate enhances adhesion and proliferation of endothelial cells: Implications for tissue engineering." *Biomacromolecules,* 8(12), 3697-3704.

Briggs, D., and Seah, M. P. (1992). *Practical Surface Analysis, Vol. 2: Ion and Neutral Spectroscopy,* 2nd Ed., Wiley, New York.

Buchholz, V., Wegner, G., Stemme, S., Ödberg, L. (1996). "Regeneration, derivatization, and utilization of cellulose in ultrathin films." *Advanced Materials,* 8(5), 399-402.

Butt, H. J. (1991). "Measuring electrostatic, van der waals, and hydration forces in electrolyte solutions with an atomic force microscope." *Biophys. J.,* 60(6), 1438-1444.

Butt, H., Cappella, B., Kappl, M. (2005). "Force measurements with the atomic force microscope: Technique, interpretation and applications." *Surface Science Reports,* 59(1-6), 1-152.

Carambassis, A., and Rutland, M. (1999). "Interactions of cellulose surfaces: Effect of electrolyte." *Langmuir,* 15(17), 5584-5590.

Cooper, G. K., Sandberg, K. R., Hinck, J. F. (1981). "Trimethylsilyl cellulose as precursor to regenerated cellulose fiber." *J Appl Polym Sci,* 26(11), 3827-3836.

De Souza Lima, M., and Borsali, R. (2004). "Rodlike cellulose microcrystals: Structure, properties, and applications." *Macromolecular Rapid Communications,* 25(7), 771-787.

Dinand, E., Chanzy, H., Vignon, M. R. (1999). "Suspensions of cellulose microfibrils from sugar beet pulp." *Food Hydrocoll.,* 13(3), 275-283.

Dinand, E., Chanzy, H., Vignon, M. R. (1996). "Parenchymal cell cellulose from sugar beet pulp: Preparation and properties." *Cellulose,* 3(3), 183-188.

Dong, X. M., Revol, J., Gray, D. G. (1998). "Effect of microcrystallite preparation conditions on the formation of colloid crystals of cellulose." *Cellulose,* 5(1), 19-32.

Dong, X. M., Kimura, T., Revol, J., Gray, D. G. (1996). "Effects of ionic strength on the isotropic-chiral nematic phase transition of suspensions of cellulose crystallites." *Langmuir,* 12(8), 2076-2082.

Donnan, F. G. (1912).“The theory of membrane equilibrium in the presence of a non-dialyzable electrolyte.“ *Z. Electrochem.,* 17, 572.

Ducker, W. A., Senden, T. J., Pashley, R. M. (1991). "Direct measurement of colloidal forces using an atomic force microscope." *Nature,* 353(6341), 239-241.

Dufresne, A., Dupeyre, D., Vignon, M. (2000). "Cellulose microfibrils from potato tuber cells: Processing and characterization of starch-cellulose microfibril composites." *J Appl Polym Sci,* 76, 2080-2092.

Edgar, C. D., and Gray, D. G. (2003). "Smooth model cellulose I surfaces from nanocrystal suspensions." *Cellulose,* 10(4), 299-306.

Enarsson, L.-E. (2008). “Dynamic and equilibrium properties of adsorbed polyelectrolyte layers.” Doctoral thesis, KTH: Stockholm.

Eriksson, J., Malmsten, M., Tiberg, F., Callisen, T. H., Damhus, T., Johansen, K. S. (2005). "Enzymatic degradation of model cellulose films." *J. Colloid Interface Sci.,* 284(1), 99-106.

Eriksson, M. (2006). "The influence of molecular adhesion on paper strength." Doctoral thesis, KTH: Stockholm.

Espy, H. H. (1995). "The mechanism of wet-strength development in paper: A review." *Tappi J.,* 78(4), 90-99.

Fleming, K., Gray, D. G., Matthews, S. (2001). "Cellulose crystallites." *Chemistry -A European Journal,* 7(9), 1831-1835.

Fleming, K., Gray, D., Prasannan, S., Matthews, S. (2000). "Cellulose crystallites: A new and robust liquid crystalline medium for the measurement of residual dipolar couplings." *J. Am. Chem. Soc.,* 122(21), 5224-5225.

Fält, S., Wågberg, L., Vesterlind, E. (2003). "Swelling of model films of cellulose having different charge densities and comparison to the swelling behavior of corresponding fibers." *Langmuir,* 19(19), 7895-7903.

Geffroy, C., Labeau, M. P., Wong, K., Cabane, B., Cohen Stuart, M. A. (2000). "Kinetics of adsorption of poly(vinylamine) onto cellulose." *Colloids and Surfaces, A: Physicochemical and Engineering Aspects,* 172(1-3), 47-56.

Greber, G., and Paschinger, O. (1981). "Silyl derivates of cellulose." *Papier,* 35(12), 547-554.

Grignon, J., and Scallan, A. M. (1980). "Effect of pH and neutral salts upon the swelling of cellulose gels." *J Appl Polym Sci,* 25(12), 2829-2843.

Grunert, M., and Winter, W. T. (2002). "Nanocomposites of cellulose acetate butyrate reinforced with cellulose nanocrystals." *Journal of Polymers and the Environment,* 10(1/2), 27-30.

Gunnars, S., Wågberg, L., Cohen Stuart, M. A. (2002). "Model films of cellulose: I. Method development and initial results." *Cellulose,* 9, 239.

Gärdlund, L., Wågberg, L., Gernandt, R. (2003). "Polyelectrolyte complexes for surface modification of wood fibres. II. Influence of complexes on wet and dry strength of paper." *Colloids and Surfaces, A: Physicochemical and Engineering Aspects,* 218(1-3), 137-149.

Habibi, Y., Foulon, L., Aguie-Beghin, V., Molinari, M., Douillard, R. (2007). "Langmuir-Blodgett films of cellulose nanocrystals: Preparation and characterization." *J. Colloid Interface Sci.,* 316(2), 388-397.

Hamad, W. (2006). "On the development and applications of cellulosic nanofibrillar and nanocrystalline materials." *Can. J. Chem. Eng.,* 84(5), 513-519.

Herrick, F. W., Casebier, R. L., Hamilton, J. K., Sandberg, K. R. (1983). "Microfibrillated cellulose: Morphology and accessibility." *J. Appl. Polym. Sci.: Appl. Polym. Symp.,* 37, 797.

Heux, L., Chauve, G., Bonini, C. (2000). "Nonflocculating and chiral-nematic self-ordering of cellulose microcrystals suspensions in nonpolar solvents." *Langmuir,* 16(21), 8210-8212.

Heux, L., Dinand, E., Vignon, M. R. (1999). "Structural aspects in ultrathin cellulose microfibrils followed by 13C CP-MAS NMR." *Carbohydr. Polym.,* 40(2), 115-124.

Himmel, M. E., Ding, S., Johnson, D. K., Adney, W. S., Nimlos, M. R., Brady, J. W., Foust, T. D. (2007). "Biomass recalcitrance: Engineering plants and enzymes for biofuels production." *Science,* 315(5813), 804-807.

Holmberg, M., Berg, J., Stemme, S., Ödberg, L., Rasmusson, J., Claesson, P. (1997). "Surface force studies of Langmuir-Blodgett cellulose films." *J. Colloid Interface Sci.,* 186(2), 369-381.

Hubbe, M. A., Rojas, O. J., Lucia, L. A., Sain, M. (2008). "Cellulosic nanocomposites: A review." *BioResources,* 3(3), 929-980.

Hult, E., Larsson, P. T., Iversen, T. (2001). "Cellulose fibril aggregation - an inherent property of kraft pulps." *Polymer,* 42(8), 3309-3314.

Höök, F., Rodahl, M., Brzezinski, P., Kasemo, B. (1998). "Energy dissipation kinetics for protein and antibody-antigen adsorption under shear oscillation on a quartz crystal microbalance." *Langmuir,* 14(4), 729-734.

Iwamoto, S., Abe, K., Yano, H. (2008). "The effect of hemicelluloses on wood pulp nanofibrillation and nanofiber network characteristics." *Biomacromolecules,* 9(3), 1022-1026.

Iwamoto, S., Nakagaito, A. N., Yano, H., Nogi, M. (2005). "Optically transparent composites reinforced with plant fiber-based nanofibers." *Appl. Phys. A,* 81(6), 1109-1112.

Jakob, H. F., Fengel, D., Tschegg, S. E., Fratzl, P. (1995). "The elementary cellulose fibril in picea abies: Comparison of transmission electron microscopy, small-angle X-ray scattering, and wide-angle X-ray scattering results." *Macromolecules,* 28(26), 8782-8787.

Johannsmann, D., Mathauer, K., Wegner, G., Knoll, W. (1992). "Viscoelastic properties of thin films probed with a quartz-crystal resonator." *Phys. Rew. B,* 46(12), 7808-7815.

Josefsson, P., Henriksson, G., Wågberg, L. (2008). "The physical action of cellulases revealed by a quartz crystal microbalance study using ultrathin cellulose films and pure cellulases." *Biomacromolecules,* 9(1) 249-254.

Kim, J., Montero, G. A., Wang, X., Argyropoulos, D. S., Genzer, J., Hinestroza, J. P., Rojas, O. J. (2006). *High-performance nanofibers and nanostructures for new generation multifunctional materials*, Proceedings of the 2006 AIChE annual meeting, San Francisco, CA.

Klemm, D., Schumann, D., Kramer, F., Hessler, N., Hornung, M., Schmauder, H., Marsch, S. (2006). "Nanocelluloses as innovative polymers in research and application." *Advances in Polymer Science,* 205(Polysaccharides II), 49-96.

Klemm, D., Schumann, D., Udhardt, U., Marsch, S. (2001). "Bacterial synthesized cellulose - artificial blood vessels for microsurgery." *Progress in Polymer Science,* 26(9), 1561-1603.

Kontturi, E., Thüne, P. C., Niemantsverdriet, J. W. (2003). "Novel method for preparing cellulose model surfaces by spin coating." *Polymer,* 44(13), 3621-3625.

Kontturi, E., Johansson, L., Kontturi, K. S., Ahonen, P., Thüne, P. C., Laine, J. (2007). "Cellulose nanocrystal submonolayers by spin coating." *Langmuir,* 23(19), 9674-9680.

Kontturi, E., Tammelin, T., Österberg, M. (2006). "Cellulose-model films and the fundamental approach." *Chem. Soc. Rev.,* 35(12), 1287-1304.

Kontturi, K. S., Tammelin, T., Johansson, L., Stenius, P. (2008). "Adsorption of cationic starch on cellulose studied by QCM-D." *Langmuir,* 24(9), 4743-4749.

Laine, J., Lindström, T., Nordmark, G. G., Risinger, G. (2002). "Studies on topochemical modification of cellulosic fibres. Part 3. The effect of carboxymethyl cellulose attachment on wet-strength development by alkaline-curing polyamide-amine epichlorohydrin resins." *Nordic Pulp & Paper Research Journal,* 17(1), 57-60.

Laine, J., Lindström, T., Nordmark, G. G., Risinger, G. (2000). "Studies on topochemical modification of cellulosic fibers. Part 1. chemical conditions for the attachment of carboxymethyl cellulose onto fibers." *Nordic Pulp & Paper Research Journal,* 15(5), 520-526.

Laine, J., Lövgren, L., Stenius, P., Sjöberg, S. (1994). "Potentiometric titration of unbleached kraft cellulose fiber surfaces." *Colloids and Surfaces, A: Physicochemical and Engineering Aspects,* 88(2-3), 277-287.

Langmuir, I., and Schaefer, V. J. (1938). "Activities of urease and pepsin monolayers." *J. Am. Chem. Soc.,* 60, 1351-1360.

Langmuir, I. (1917). "Constitution and fundamental properties of solids and liquids. II. liquids." *J. Am. Chem. Soc.,* 39, 1848-1906.

Larson, R. G., and Rehg, T. (1997). In *Liquid Film Coating,* Kistler, S. F.; Schweizer, P. M., eds, Chapman & Hall, London, Ch 14.

Lowys, M., Desbrieres, J., Rinaudo, M. (2001). "Rheological characterization of cellulosic microfibril suspensions. role of polymeric additives." *Food Hydrocoll.,* 15(1), 25-32.

Lu, J., Askeland, P., Drzal, L. T. (2008). "Surface modification of microfibrillated cellulose for epoxy composite applications." *Polymer,* 49(5), 1285-1296.

Luner, P., and Sandell, M. (1969). "The wetting of cellulose and wood hemicelluloses." *J. Polym. Sci. , Part C: Polym. Symp.,* 28, 115.

Marchessault, R. H., Morehead, F. F., Koch, M. J. (1961). "Hydrodynamic properties of neutral suspensions of cellulose crystallites as related to size and shape." *J. Colloid Sci.,* 16, 327-344.

Marchessault, R. H., Morehead, F. F., Walter, N. M. (1959). "Liquid crystal systems from fibrillar polysaccharides." *Nature,* 184 (Suppl. No. 9), 632-633.

McCrackin, F. L., Passaglia, E., Stromberg, R. R., Steinberg, H. L. (1963). "Measurement of the thickness and refractive index of very thin films and the optical properties of surfaces by ellipsometry." *J.Res. Natl. Bur. Std.,* A67(4), 363-377.

McNeal, M. R., Nanko, H., Hubbe, M. A. (2005). "Imaging of macromolecular events occurring during the manufacture of paper." Advances in Paper Science and Technology: 13th fundamental research symposium, Cambridge, UK.

Müller, M., Czihak, C., Schober, H., Nishiyama, Y., Vogl, G. (2000). "All disordered regions of native cellulose show common low-frequency dynamics." *Macromolecules,* 33(5), 1834-1840.

Naderi, A., and Claesson, P. M. (2006). "Adsorption properties of polyelectrolyte-surfactant complexes on hydrophobic surfaces studied by QCM-D." *Langmuir,* 22(18), 7639-7645.

Nakagaito, A. N., and Yano, H. (2005). "Novel high-strength biocomposites based on microfibrillated cellulose having nano-order-unit web-like network structure." *Appl. Phys. A,* 80(1), 155-159.

Nakagaito, A. N., and Yano, H. (2004). "The effect of morphological changes from pulp fiber towards nano-scale fibrillated cellulose on the mechanical properties of high-strength plant fiber based composites." *Appl. Phys. A,* 78(4), 547-552.

Nehls, I., Wagenknecht, W., Philipp, B., Stscherbina, D. (1994). "Characterization of cellulose and cellulose derivatives in solution by high resolution carbon-13 NMR spectrometry." *Progress in Polymer Science,* 19(1), 29-78.

Neuman, R. D., Berg, J. M., Claesson, P. M. (1993). ”Direct measurement of surface forces in papermaking and paper coating systems.” *Nordic Pulp Paper Res. J.,* 8, 96.

Nogi, M., and Yano, H. (2008). "Transparent nanocomposites based on cellulose produced by bacteria offer potential innovation in the electronics device industry." *Advanced Materials,* 20(10), 1849-1852.

Nogi, M., Handa, K., Nakagaito, A. N., Yano, H. (2005). "Optically transparent bionanofiber composites with low sensitivity to refractive index of the polymer matrix." *Appl. Phys. Lett.,* 87(24), 243110/1-243110/3.

Nordgren, N., Eklöf, J., Zhou, Q., Brumer, H., Rutland, M. W. (2008). "Top-down grafting of xyloglucan to gold monitored by QCM-D and AFM: Enzymatic activity and interactions with cellulose." *Biomacromolecules,* 9(3), 942-948.

Norrman, K., Ghanbari-Siahkali, A., Larsen, N. B. (2005). "Studies of spin-coated polymer films." *Annual Reports on the Progress of Chemistry, Section C: Physical Chemistry,* 101, 174-201.

Notley, S. (2008). "Effect of introduced charge in cellulose gels on surface interactions and the adsorption of highly charged cationic polyelectrolytes." *Physical Chemistry Chemical Physics,* 10(13), 1819-1825.

Notley, S., Eriksson, M., Wågberg, L., Beck, S., Gray, D. (2006). "Surface forces measurements of spin-coated cellulose thin films with different crystallinity." *Langmuir,* 22(7), 3154-3160.

Notley, S., and Wågberg, L. (2005). "Morphology of modified regenerated model cellulose II surfaces studied by atomic force microscopy: Effect of carboxymethylation and heat treatment." *Biomacromolecules,* 6(3), 1586-1591.

Notley, S., Pettersson, B., Wågberg, L. (2004). "Direct measurement of attractive van der Waals' forces between regenerated cellulose surfaces in an aqueous environment." *J. Am. Chem. Soc.,* 126(43), 13930-13931.

Ono, H., Shimaya, Y., Sato, K., Hongo, T. (2004). "H spin-spin relaxation time of water and rheological properties of cellulose nanofiber dispersion, transparent cellulose hydrogel (TCG)." *Polymer Journal,* 36(9), 684-694.

O'Sullivan, A. C. (1997). "Cellulose: The structure slowly unravels." *Cellulose,* 4(3), 173.

Ozin, G. A., and Arsenault, A. C. (2005). *Nanochemistry: A Chemical Approach to Nanomaterials,* The royal society of chemistry, Cambridge, UK.

Österberg, M., and Claesson, P. M. (2000). "Interactions between cellulose surfaces: Effect of solution pH." *J. Adhes. Sci. Technol.,* 14(5), 603-618.

Penfold, J., Tucker, I., Petkov, J., Thomas, R. K. (2007). "Surfactant adsorption onto cellulose surfaces." *Langmuir,* 23(16), 8357-8364.

Poptoshev, E., Carambassis, A., Österberg, M., Claesson, P. M., Rutland, M. W. (2000). "Comparison of model surfaces for cellulose interactions: Elevated pH." *Progress in Colloid & Polymer Science,* 116 (Surface and Colloid Science), 79-83.

Poptoshev, E., and Claesson, P. M. (2002). "Weakly charged polyelectrolyte adsorption to glass and cellulose studied by surface force technique." *Langmuir*, 18(4), 1184-1189.

Revol, J., Bradford, H., Giasson, J., Marchessault, R. H., Gray, D. G. (1992). "Helicoidal self-ordering of cellulose microfibrils in aqueous suspension." *Int. J. Biol. Macromol.,* 14(3), 170-172.

Revol, J. F., Godbout, L., Dong, X. M., Gray, D. G., Chanzy, H., Maret, G. (1994). "Chiral nematic suspensions of cellulose crystallites; phase separation and magnetic field orientation." *Liquid Crystals,* 16(1), 127-134.

Rodahl, M., Höök, F., Krozer, A., Brzezinski, P., Kasemo, B. (1995). "Quartz crystal microbalance setup for frequency and Q-factor measurements in gaseous and liquid environments." *Rev. Sci. Instrum.,* 66(7), 3924-3930.

Rojas, O. J., Jeong, C., Turon, X., Argyropoulos, D. S. (2007). "Measurement of cellulase activity with piezoelectric resonators." *ACS Symp. Ser.,* 954 (Materials, Chemicals, and Energy from Forest Biomass), 478-494.

Rudraraju, V. S., and Wyandt, C. M. (2005a). "Rheology of microcrystalline cellulose and sodiumcarboxymethyl cellulose hydrogels using a controlled stress rheometer: Part II." *Int. J. Pharm.,* 292(1-2), 63-73.

Rudraraju, V. S., and Wyandt, C. M. (2005b). "Rheological characterization of microcrystalline Cellulose/Sodiumcarboxymethyl cellulose hydrogels using a controlled stress rheometer: Part I." *Int. J. Pharm.,* 292(1-2), 53-61.

Rånby, B. G. (1951). "The colloidal properties of cellulose micelles." *Discuss. Faraday Soc.,* No. 11, 158-164, discussion 208-213.

Saarinen, T., Österberg, M., Laine, J. (2009). "Properties of cationic polyelectrolyte layers adsorbed on silica and cellulose surfaces studied by QCM-D - effect of polyelectrolyte charge density and molecular weigth." *J. Dispersions Science Technology,* 30(6), 27.

Saito, T., Kimura, S., Nishiyama, Y., Isogai, A. (2007). "Cellulose nanofibers prepared by TEMPO-mediated oxidation of native cellulose." *Biomacromolecules,* 8(8), 2485-2491.

Salmi, J., Österberg, M., Laine, J. (2007). "The effect of cationic polyelectrolyte complexes on interactions between cellulose surfaces." *Colloids and Surfaces, A: Physicochemical and Engineering Aspects,* 297(1-3), 122-130.

Sauerbrey, G. (1959). "The use of quartz oscillators for weighing thin layers and for microweighing." *Zeitschrift Für Physik,* 155, 206-222.

Schasfoort, R., and Tudos, A. (2008). *Handbook of Surface Plasmon Resonance,* The Royal Society of Chemistry, RSC Publishing.

Schaub, M., Wenz, G., Wegner, G., Stein, A., Klemm, D. (1993). *Adv. Mater.,* (5), 919.

Sjöström, E. (1993). *Wood Chemistry: Fundamentals and Applications,* Academic Press Inc., San Diego, USA.

Stenstad, P., Andresen, M., Tanem, B. S., Stenius, P. (2008). "Chemical surface modifications of microfibrillated cellulose." *Cellulose,* 15(1), 35-45.

Stiernstedt, J., Nordgren, N., Wågberg, L., Brumer, H., Gray, D. G., Rutland, M. W. (2006). "Friction and forces between cellulose model surfaces: A comparison." *J. Colloid Interface Sci.,* 303(1), 117-123.

Subramanian, R., Kononov, A., Kang, T., Paltakari, J., Paulapuro, H. (2008). "Structure and properties of some natural cellulosic fibrils." *BioResources,* 3(1), 192-203.

Svensson, A., Nicklasson, E., Harrah, T., Panilaitis, B., Kaplan, D. L., Brittberg, M., Gatenholm, P. (2005). "Bacterial cellulose as a potential scaffold for tissue engineering of cartilage." *Biomaterials,* 26(4), 419-431.

Swerin, A., and Wågberg, L. (1994). "Size-exclusion chromatography for characterization of cationic polyelectrolytes used in papermaking." *Nordic Pulp & Paper Research Journal,* 9(1), 18-25.

Taiz, L., and Zeiger, E. (2002). *Plant Physiology,* Sinauer Associates, Inc., Sunderland, USA.

Tammelin, T., Johnsen, I. A., Österberg, M., Stenius, P., Laine, J. (2007). "Adsorption of colloidal extractives and dissolved hemicelluloses on thermomechanical pulp fiber components studied by QCM-D." *Nordic Pulp & Paper Research Journal,* 22(1), 93-101.

Tammelin, T., Saarinen, T., Österberg, M., Laine, J. (2006). "Preparation of Langmuir/Blodgett-cellulose surfaces by using horizontal dipping procedure. application for polyelectrolyte adsorption studies performed with QCM-D." *Cellulose,* 13(5), 519-535.

Taniguchi, T., and Okamura, K. (1998). "New films produced from microfibrillated natural fibres." *Polym. Int.,* 47, 291-294.

Tatsumi, D., Ishioka, S., Matsumoto, T. (2002). "Effect of fiber concentration and axial ratio on the rheological properties of cellulose fiber suspensions." *Journal of the Society of Rheology, Japan,* 30(1), 27-32.

Torn, L. H., Koopal, L. K., de Keizer, A., Lyklema, J. (2005). "Adsorption of nonionic surfactants on cellulose surfaces: Adsorbed amounts and kinetics." *Langmuir,* 21(17), 7768-7775.

Turbak, A. F., Snyder, F.,W., Sandberg, K. R. (1983). "Microfibrillated cellulose, a new cellulose product: Properties, uses, and commercial potential." *J. Appl. Polym. Sci. : Appl. Polym. Symp.,* 37, 813.

Turon, X., Rojas, O. J., Deinhammer, R. S. (2008). "Enzymatic kinetics of cellulose hydrolysis: A QCM-D study." *Langmuir,* 24(8), 3880-3887.

Van de Ven, T. (2000). "A model for the adsorption of polyelectrolytes on pulp fibers: Relation between fiber structure and polyelectrolyte properties." *Nordic Pulp & Paper Research Journal,* 15(5), 494-501.

Wågberg, L., Decher, G., Norgren, M., Lindström, T., Ankerfors, M., Axnäs, K. (2008). "The build-up of polyelectrolyte multilayers of microfibrillated cellulose and cationic polyelectrolytes." *Langmuir,* 24(3), 784-795.

Wågberg, L. (2000). "Polyelectrolyte adsorption onto cellulose fibers - a review." *Nordic Pulp & Paper Research Journal,* 15(5), 586-597.

Wågberg, L., and Björklund, M. (1993). "On the mechanism behind wet strength development in papers containing wet strength resins." *Nordic Pulp & Paper Research Journal,* 8(1), 53-58.

Whitesides, G. M. (2005). "Nanoscience, nanotechnology, and chemistry." *Small,* 1(2), 172-179.

Williams, D. B., and Carter, B. C. (1996). *Transmission Electron Microscopy: A Textbook for Materials Science,* Plenum Press, New York.

Yan, H., Lindström, T., Christiernin, M. (2006). "Some ways to decrease fibre suspension flocculation and improve sheet formation." *Nordic Pulp & Paper Research Journal,* 21(1), 36-43.

Yokota, S., Kitaoka, T., Sugiyama, J., Wariishi, H. (2007). "Cellulose I nanolayers designed by self-assembly of its thiosemicarbazone on a gold substrate." *Advanced Materials,* 19(20), 3368-3370.

Zhong, Q., Inniss, D., Kjoller, K., Elings, V. B. (1993). "Fractured polymer/silica fiber surface studied by tapping mode atomic force microscopy." *Surf Sci,* 290(1-2), L688-L692.

Zhou, Q., Rutland, M. W., Teeri, T. T., Brumer, H. (2007). "Xyloglucan in cellulose modification." *Cellulose,* 14(6), 625-641.

Zuluaga, R., Putaux, J., Restrepo, A., Mondragon, I., Ganan, P. (2007). "Cellulose microfibrils from banana farming residues: Isolation and characterization." *Cellulose,* 14(6), 585-592.

TKK REPORTS IN FOREST PRODUCTS TECHNOLOGY, SERIES A

A1. Subramanian R.,
Engineering fine paper by utilising the structural elements of the raw materials. Doctoral Thesis. 2008.

A2. Haapio A.,
Environmental assessment of buildings. Doctoral Thesis. 2008.

A3. El-Sarkawy K.,
Different approaches to tailoring chemical pulp fibres. Doctoral Thesis. 2008.

ISSN 1797-4496

ISBN 978-951-22-9648-4

Picaset Oy, Helsinki 2008